nature COMMUNICATIONS

ARTICLE

Received 24 Nov 2013 | Accepted 9 May 2014 | Published 18 Jun 2014

DOI: 10.1038/ncomms5081 OPEN

Cell cycle transition from S-phase to G1 in *Caulobacter* is mediated by ancestral virulence regulators

Coralie Fumeaux[1], Sunish Kumar Radhakrishnan[1,†], Silvia Ardissone[1], Laurence Théraulaz[1], Antonio Frandi[1], Daniel Martins[1], Jutta Nesper[2], Sören Abel[2,†], Urs Jenal[2] & Patrick H. Viollier[1]

Zinc-finger domain transcriptional regulators regulate a myriad of functions in eukaryotes. Interestingly, ancestral versions (MucR) from Alpha-proteobacteria control bacterial virulence/symbiosis. Whether virulence regulators can also control cell cycle transcription is unknown. Here we report that MucR proteins implement a hitherto elusive primordial S→G1 transcriptional switch. After charting G1-specific promoters in the cell cycle model *Caulobacter crescentus* by comparative ChIP-seq, we use one such promoter as genetic proxy to unearth two MucR paralogs, MucR1/2, as constituents of a quadripartite and homeostatic regulatory module directing the S→G1 transcriptional switch. Surprisingly, MucR orthologues that regulate virulence and symbiosis gene transcription in *Brucella*, *Agrobacterium* or *Sinorhizobium* support this S→G1 switch in *Caulobacter*. Pan-genomic ChIP-seq analyses in *Sinorhizobium* and *Caulobacter* show that this module indeed targets orthologous genes. We propose that MucR proteins and possibly other virulence regulators primarily control bacterial cell cycle (G1-phase) transcription, rendering expression of target (virulence) genes periodic and in tune with the cell cycle.

[1] Department Microbiology and Molecular Medicine, Faculty of Medicine/CMU, Institute of Genetics and Genomics in Geneva (iGE3), University of Geneva, Rue Michel Servet 1, 1211 Genève 4, Switzerland. [2] Biozentrum of the University of Basel, Klingelbergstrasse 50/70, 4056 Basel, Switzerland. † Present addresses: Indian Institute of Science Education and Research, CET campus, Thiruvananthapuram 695016, Kerala, India (S.K.R.); Division of Infectious Diseases, Department of Microbiology and Immunobiology, Brigham and Women's Hospital, Harvard Medical School, 181 Longwood Avenue, Boston, Massachusetts 02115, USA (S.A.). Correspondence and requests for materials should be addressed to P.H.V. (email: Patrick.Viollier@unige.ch).

How S-phase cells instate the G1-phase transcriptional programme is poorly understood. The synchronizable Alpha-proteobacterium *Caulobacter crescentus* (henceforth *Caulobacter*) is the pre-eminent model system commonly used to dissect cell cycle transcription at the most fundamental level[1,2]. *Caulobacter* divides into a smaller and motile swarmer cell and a larger and sessile stalked cell, residing in G1- and S-phase, respectively (Fig. 1a). Such asymmetric division has also been reported for related Alpha-proteobacterial pathogens/symbionts[3] belonging to the genera *Brucella*, *Agrobacterium* or *Sinorhizobium,* some of which are also synchronizable[4,5]. As Alpha-proteobacteria generally encode most known cell cycle regulatory proteins originally identified in *Caulobacter*[6], the underlying mechanisms for the G1-phase transcriptional programme seem to be conserved and perhaps serve to control expression of virulence/symbiosis functions as a function of the cell cycle. Indeed, virulence functions are typically present in non-replicative dispersal cell types of unrelated pathogens such as members of the *Chlamydiae*[7], and features of an underlying cytological and/or molecular asymmetry have also been reported for the pathogenic Gamma-proteobacteria *Pseudomonas aeruginosa* and *Klebsiella pneumoniae*[8] and distantly related mycobacteria[9]. This suggests that the implementation of daughter cell-specific transcriptional programs is pervasive among different prokaryotic lineages, and that lineage-specific mechanisms direct this re-programming.

In *Caulobacter*, the two daughter cell types can be conveniently discerned based on functional and morphological criteria: while the G1-phase cell harbours several adhesive pili and a single flagellar motor at the old pole, the S-phase cell harbours a stalk with an adhesive holdfast at the corresponding pole. In addition, these two cell types differ in their buoyancy, a feature that is exploited for the enrichment of a pure population of G1 cells on a density gradient[10]. A hallmark of the *Caulobacter* G1→S transition is the loss of the flagellum and pili, the elaboration of a stalk and holdfast, as well as the switch in cellular buoyancy. In the ensuing S-phase, cells segregate the replicated DNA, activate motility genes and assemble the flagellar motor and pilus secretion apparatus at the pole opposite the stalk[1]. As soon as the pre-divisional cell compartmentalizes, the G1-phase transcriptional programme is instated in the swarmer chamber, pili are extruded, the flagellum is energized and the cellular buoyancy is reversed. In the stalked chamber, DNA replication re-initiates and S-phase transcription resumes.

How the switch from S-phase to the G1-phase transcriptional programme (henceforth referred to as S→G1 transcriptional switch) is induced at compartmentalization is unresolved. P_{pilA}, the promoter of the gene encoding the structural component of the pilus filament (*pilA)*, is a target of this regulation and thus suitable as genetic proxy. P_{pilA} is activated in G1-phase[11] by the conserved and essential cell cycle transcriptional regulator A (CtrA)[12]. CtrA can function either as activator or repressor of transcription and also as an inhibitor of DNA replication by directly binding the TTAA-N(7)-TTAA target motif (CtrA box) in promoters and the origin of replication, *Cori*[1]. Binding of CtrA to its targets is enhanced by phosphorylation (CtrA∼P) of aspartate 51 (D51) by way of a complex phosphorelay involving the conserved and essential hybrid histidine kinase CckA[13]. CtrA is proteolytically removed during the G1→S transition, re-synthesized and again proteolysed by the ClpXP protease in the nascent S-phase chamber upon compartmentalization[1] (Fig. 1a). Thus, CtrA is not a G1-specific regulator as it is already present and active before compartmentalization (that is, in late S-phase), for example, at promoters of early (class II) flagellar and other motility genes[1,14]. Determinants other than CtrA∼P likely promote the switch from S→G1 phase transcription of CtrA-dependent genes during compartmentalization[15,16].

A candidate for such an accessory role is the conserved helix-turn-helix motif protein SciP that accumulates in G1-phase[17,18]. SciP binds CtrA directly and impairs CtrA's ability to recruit RNA polymerase (RNAP) holoenzyme to $P_{pilA}$and other CtrA-activated promoters *in vitro*, apparently without establishing sequence-specific contacts to DNA[18,19]. An alternative view holds that SciP does not require CtrA to bind DNA. Instead, SciP was proposed to bind DNA directly at the 5′-TGTCGCG-3′ motif in the *ctrA* promoter *in vitro*[17]. Surprisingly, the occurrence of this motif (>1,460 predicted sites in the 4.01 Mbp GC-rich *Caulobacter* genome) vastly exceeds the number of previously predicted CtrA target promoters with 1–4 CtrA boxes (∼50)[1]. Also, mutation of the 5′-TGTCGCG-3′ motif did not affect binding of CtrA and SciP to P_{pilA} *in vitro*[19]. As both models posit that SciP targets all CtrA-dependent promoters, further investigations on the S→G1 transcriptional switch and on the possible role of SciP in this event are warranted.

Here we report a system-level and forward genetic approach for the dissection of this transcriptional switch. We unearth two uncharacterized ancestral zinc-finger domain proteins, MucR1 and MucR2, as key determinants of a novel quadripartite and homeostatic regulatory module that together with CtrA and SciP turn on G1-phase genes and concomitantly shut off S-phase genes, respectively. Using pan-genomic ChIP-seq (chromatin immunoprecipitation coupled to deep-sequencing), we reveal MucR as a direct regulator of orthologous genes in *Sinorhizobium* that can direct cell cycle transcription in *Caulobacter*. Thus, a conserved genetic module uses an ancestral transcription factor fold, extensively researched in the eukaryotic domain of life[20], to integrate virulence, symbiosis and/or cell cycle transcription in a bacterial lineage from which eukaryotic organelles descended[21].

Results

Target promoters of the S→G1 transcriptional switch. Before surveying the extent of the S→G1 promoter switch on a genome-wide scale, we first characterized candidate promoters by quantitative ChIP (qChIP) following precipitation with polyclonal antibodies to CtrA and monoclonal antibodies to the RpoC (β′) subunit of RNAP from chromatin of wild-type (*WT*) and Δ*pleC* cells. *pleC* encodes a histidine kinase/phosphatase that partitions with the G1-phase progeny (Fig. 1a) and is required for the accumulation of G1-specific transcripts, including *pilA*, and for maximal accumulation of CtrA∼P[15]. qChIP confirmed that CtrA and RNAP occupancy at P_{pilA} are 58 and 48% less abundant in Δ*pleC* cells compared with *WT* cells (Fig. 1b), consistent with the reduced P_{pilA} activity (Fig. 1b–d). We also noted a similar reduction in CtrA occupancy at $P_{tacA,}$(the promoter of the G1-phase gene *tacA*), along with a commensurate reduction in promoter activity (as determined using the P_{tacA}-*lacZ* promoter-probe reporter, Supplementary Fig. 1A). By contrast, CtrA abundance at P_{fliL} (the promoter of the class II flagellar gene *fliL*) was not noticeably affected (Fig. 1e). Knowing that *fliL* mRNA peaks in late S-phase (∼84 min), that the *pilA* and *tacA* mRNAs surge in G1 (∼120 min (ref. 16)) and that PilA accumulation is PleC-dependent (Fig. 1f), we hypothesized that PleC-dependent CtrA (PleC:CtrA) target promoters regulate G1-phase genes.

Next, we charted other PleC:CtrA target promoters on a genome-wide scale by comparative ChIP-seq of CtrA occupancy in *WT* and Δ*pleC* cells. Bioinformatic analyses predicted >100 CtrA target sites that, akin to P_{pilA}, are bound substantially less efficiently by CtrA (that is, with $\log_2$ difference of < -0.8) in

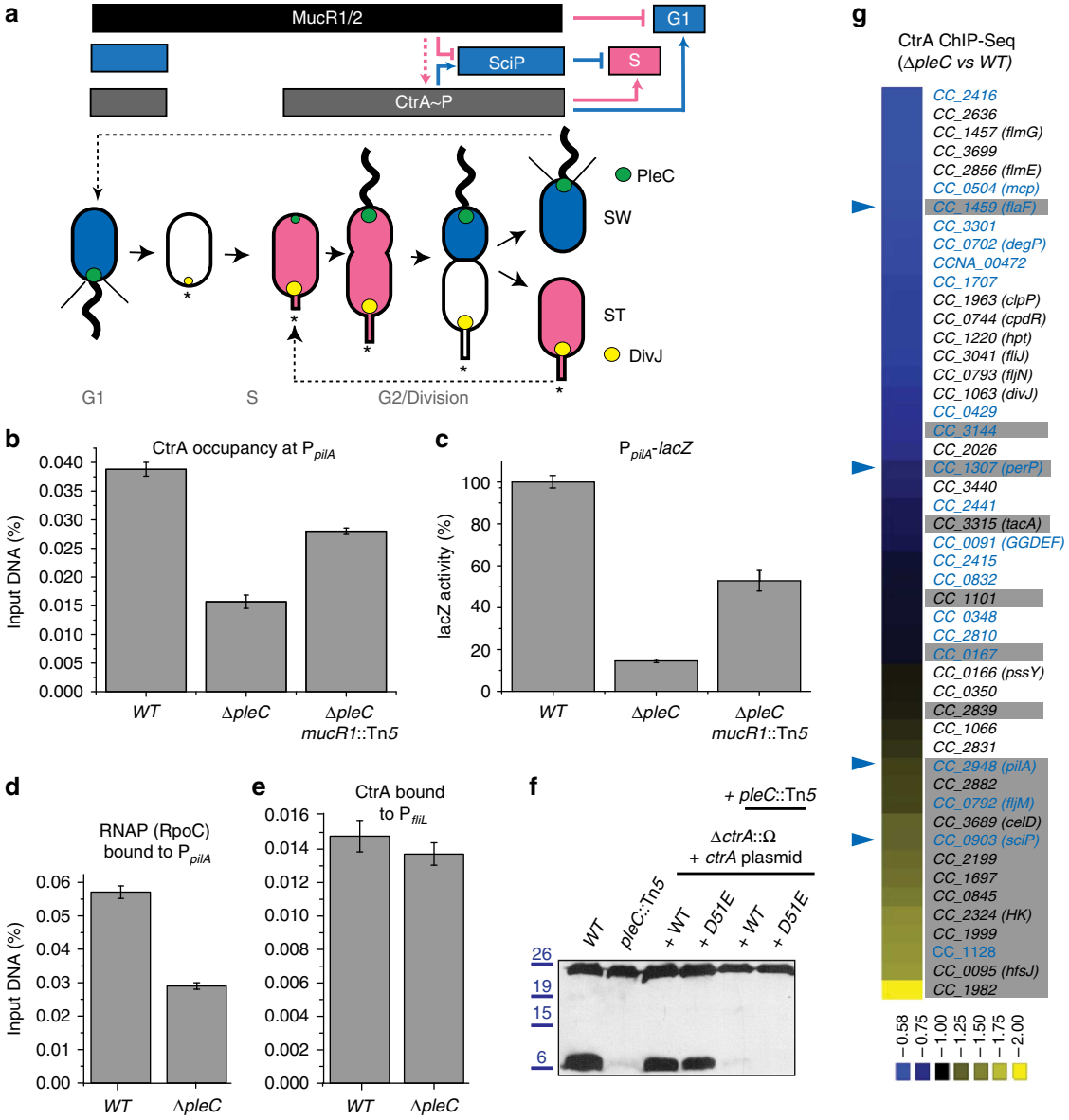

Figure 1 | CtrA-bound promoters that are affected in Δ*pleC* cells. (**a**) Schematic of the regulatory interactions between *ctrA*, *sciP* and *mucR1* and *mucR2* (*mucR1/2*) during the *C. crescentus* cell cycle. Phosphorylated CtrA (CtrA∼P) activates transcription of S- and G1-phase genes. In S-phase, MucR1/2 represses G1-genes such as *sciP*. The *sciP* gene is activated in G1 and the newly synthesized SciP translation product represses S-phase promoters. The antagonistic kinase/phosphatase pair, DivJ (yellow dot) and PleC (green dot) indirectly influence CtrA∼P and partition with the stalked (ST) cell chamber or swarmer (SW) cell chamber, respectively. PleC promotes CtrA∼P accumulation in the SW cell. The dashed arrow indicates that MucR1/2 promote expression of CtrA, but not necessarily its phosphorylation. The star denotes the holdfast. Blue colouring denotes G1-phase transcription, whereas pink is for the late S-phase programme. Light grey labels indicate the cell cycle stages. (**b**–**e**) Occupancy of CtrA and RNA polymerase (RNAP) at the *pilA* (P_{pilA}) and *fliL* promoter (P_{fliL}) in *WT* (NA1000), Δ*pleC* and Δ*pleC mucR1*::Tn*5* mutant cells as determined by quantitative chromatin immunoprecipitation assays (qChIP) using antibodies to CtrA or RpoC, as well as *pilA* transcription measurements conducted using a P_{pilA}-*lacZ* promoter-probe reporter. Data are from three biological replicates. Error is shown as s.d. (**f**) Immunoblots showing PilA (lower band, approximately 6 kDa) and CtrA (upper band, approximately 26 kDa) steady-state levels in *WT* and *pleC*::Tn*5* mutant cells harbouring *WT ctrA* or phosphomimetic *ctrA(D51E)* expressed from a plasmid in the absence of chromosomally encoded CtrA (Δ*ctrA*::Ω). Molecular size standards are indicated on the left as blue lines with the corresponding values (blue) in kDa. (**g**) Comparative ChIP-seq performed with antibodies to CtrA on chromatin from *WT* and Δ*pleC* cells. Boxed in grey are PleC:CtrA promoters that were verified as being PleC dependent (Supplementary Fig. 1B). Blue labels indicate PleC:CtrA promoters that are bound by MucR1/2 as determined by the ChIP-seq experiments (Fig. 2). Blue arrowheads point to promoters for which the ChIP-seq traces are shown in Fig. 5. The colour key at the bottom indicates the degree by which the occupancy of CtrA is altered by the Δ*pleC* mutation, expressed as $\log_2$ ratio (Supplementary Data 1).

Δ*pleC* versus *WT* cells (Figs 1g and 2a; and Supplementary Data 1). To confirm that these sites indeed harbour PleC:CtrA target promoters, we constructed promoter-probe reporters of the top 18 PleC:CtrA target sites and measured promoter activities in *WT* and Δ*pleC* cells (Supplementary Figs 1B and 2A,B). All reporters were less active in Δ*pleC* cells, showing that they indeed harbour PleC:CtrA target promoters. Since the transcripts produced from these promoters are restricted to G1-phase[15,22], we conclude that these sites define a new class of G1-phase promoters that are activated by CtrA in a PleC-dependent

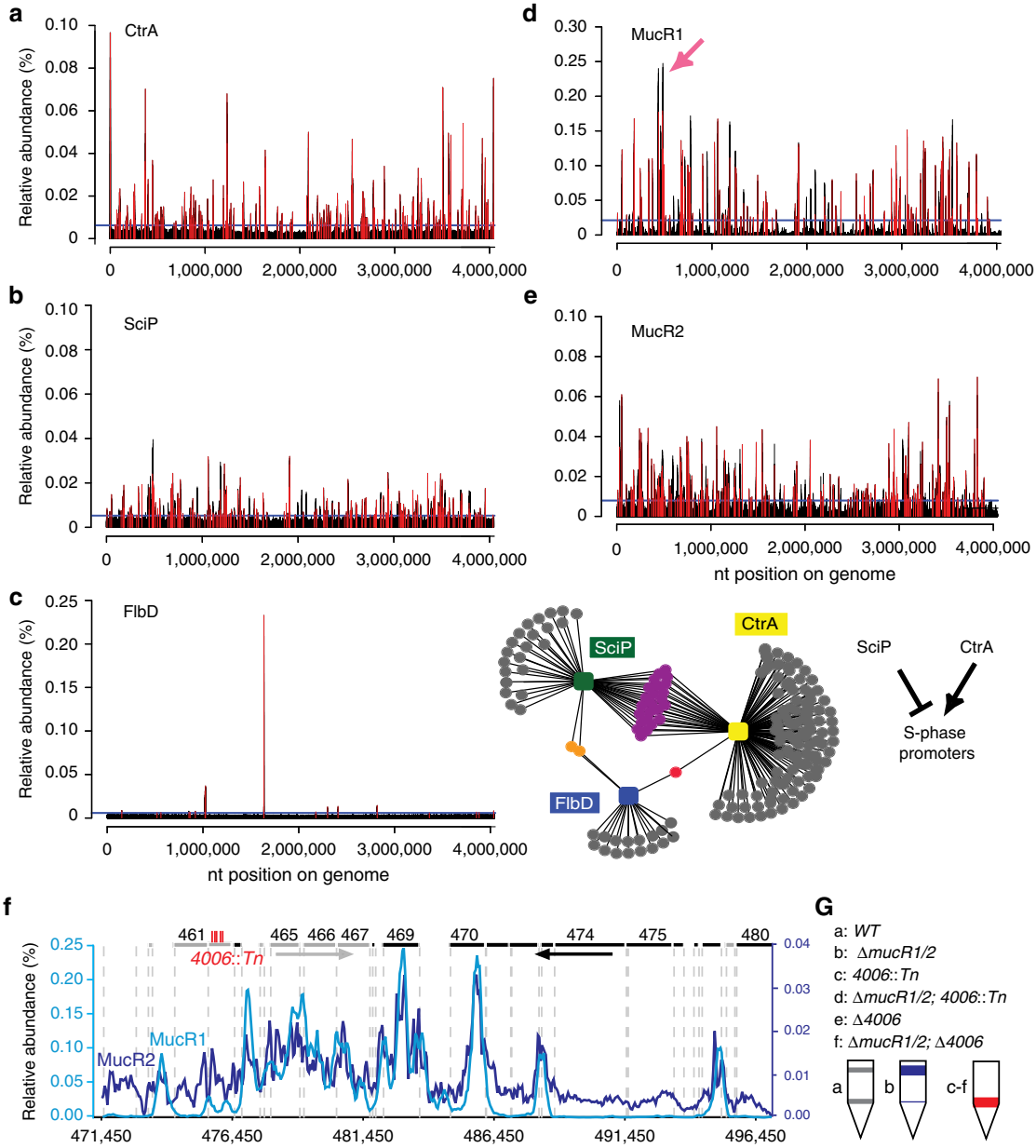

Figure 2 | Genome-wide occupancy of CtrA, SciP, FlbD, MucR1 and MucR2. (**a**–**e**). Genome-wide occupancies of CtrA (**a**), SciP (**b**), FlbD (**c**), MucR1 (**d**) and MucR2 (**e**) on the *C. crescentus* genome as determined by ChIP-seq. Note that owing to the ability of the anti-MucR2 antibody to precipitate MucR1, some of the peaks in **e** could also derive from MucR1, but this is also expected as we show in Fig. 4a that MucR1 can interact with MucR2. The *x* axis represents the nucleotide position on the genome, whereas the *y* axis denotes the relative abundance of reads for each probe (see Supplementary Methods for detailed description). Candidate peaks reported in each profile are shown as red bars ('ANNO probes'; Supplementary Data 1–5), whereas a horizontal blue line in each profile denotes the cutoff applied to separate peaks and background. The middle panel in **c** depicts the minimal overlap between the targets of SciP, CtrA and FlbD, whereas the right panel illustrates the regulatory relationship between SciP, CtrA and S-phase promoters. The pink arrow in **d** denotes the 26-kb mobile genetic element (MGE) enlarged in **f**. (**f**) ChIP-seq trace of MucR1 (light blue) and MucR2 (dark blue) on the 26-kb MGE. Genes encoded from right to left are shown in grey bars, whereas the black bars indicate genes on the reverse strand. The numbers above refer to the CCNA gene annotation. The *himar1* (*Tn*) insertions in *CCNA_04006* are shown as vertical red bars. (**g**) Buoyancy of *WT* (grey) and mutant (blue or red) cells harbouring a *himar1* (*Tn*) insertion or an in-frame deletion (Δ) in *CCNA_04006* (*4006*). The schematic shows the sedimentation of cells after Percoll density gradient centrifugation in a test tube. Although *WT* cells show the typical upper and lower buoyancy conferred by S and G1 cells, respectively, Δ*mucR1/2* cells only show the former. *CCNA_04006* is epistatic over *mucR1/2,* as inactivation *CCNA_04006* confers the latter buoyancy.

manner. Importantly, the promoter of the G1-phase gene *sciP* (P_{sciP}) also falls into this class (Supplementary Fig. 1B; see below).

SciP preferentially binds S-phase target promoters of CtrA. ChIP-seq experiments (Fig. 2b) with a polyclonal antibody to SciP revealed that SciP does not associate with *all* CtrA target sites (Fig. 2a) *in vivo*. In fact, we observed a clear promoter preference for SciP, targeting the S-phase promoters, but not G1-phase promoters activated by CtrA. Bioinformatic analyses predicted 76 SciP-binding sites *in vivo* (see Methods section and Supplementary Data 2) upstream of CtrA-activated genes whose transcripts all peak in late S-phase[16], such as flagellar genes

(for example, *flmG*, *pleA*, *fliQ*, *fliX*, *flgB*, *fliL*, *fliI* and *fljJ*), pilus secretion genes (for example, *cpaB* and others, see below) and chemotaxis gene orthologues (for example, *CC_2317*, *CC_2281* and *CC_1655*). If SciP binds DNA only through a direct association with CtrA, then *all* CtrA targets, including *Cori* and CtrA-repressed promoters, should be efficiently precipitated with the SciP antibody. These CtrA target sites as well as those of PleC:CtrA (G1) promoters such as P_{pilA} were not enriched in the ChIP sample, indicating that they are not preferred targets of SciP *in vivo* (Supplementary Discussion). A MEME-based motif search using 50 of the top SciP target sites predicted 5′-(G/A)TTAACCAT(A/G)-3′ as possible SciP consensus motif (Supplementary Data 2), a motif having half a CtrA box (underlined, see above) and often overlapping with the CtrA target site in promoters (Supplementary Data 2). These results suggest that CtrA and SciP compete for binding to these promoters, or that repression by SciP involves a cooperative binding mode between SciP and CtrA at this site, perhaps through an 'extended' CtrA box that includes a CtrA half site harbouring a SciP consensus motif. Interestingly, combinatorial promoter control by two regulators has been described during sporulation in the unrelated Delta-proteobacterium *Myxococcus xanthus*[23].

Our results also reveal that SciP binds neither P_{fliF} (the promoter of the class II flagellar gene *fliF* that is activated by CtrA in S-phase[16]) nor P_{pilA} efficiently *in vivo*. We therefore suggest that the ability of SciP to interfere with the recruitment of RNAP to CtrA∼P-activated promoters such as P_{fliF} and P_{pilA} *in vitro*[18,19] likely reflects a secondary, later-acting mechanism to silence CtrA-dependent transcription. It is conceivable that this mechanism comes into play later in G1-phase once CtrA activated transcription of *sciP* and other genes (that is, after compartmentalization) has led to a build-up of a threshold in SciP. Since our ChIP-seq experiments failed to reveal SciP at all CtrA-activated promoters, it seems that SciP binds the bipartite CtrA target complex weakly and/or only very transiently *in vivo*. The simplest interpretation of our ChIP-seq data is that SciP stably associates with promoters that CtrA activates in S-phase, while promoters that CtrA activates in G1-phase or represses (such as the *podJ* or *ftsZ* promoter) are not preferred targets of SciP *in vivo*. SciP also does not target the CtrA-bound *Cori* site or the CtrA-activated promoter P_{fliF} efficiently *in vivo*.

P_{fliF} is repressed by FlbD, the σ^{54}-dependent transcriptional activator of class III/IV and repressor of class II flagellar promoters[14]. Our ChIP-seq experiments showed that FlbD binds P_{fliF} and several other class III/IV flagellar promoters (Fig. 2c and Supplementary Fig. 3). FlbD also targets, in a mutually exclusive fashion with SciP, class II flagellar promoters (Fig. 2c and Supplementary Discussion), but neither P_{pilA} nor other PleC:CtrA target promoters.

MucR1/2 binds promoters of G1-phase genes. Our observation that phosphomimetic variants of CtrA cannot elevate P_{pilA} activity in Δ*pleC* cells (Supplementary Fig. 1C) and PilA protein accumulation, regardless of whether *WT* CtrA is present or not (Fig. 1f), predicted an unknown repressor(s) that prevents CtrA-mediated activation at P_{pilA}, P_{sciP} and other G1-promoters in Δ*pleC* cells. To identify this repressor, we mutagenized Δ*pleC* cells harbouring a P_{pilA}-*nptII* transcriptional reporter (integrated at the chromosomal *pilA* locus; *pilA*::P_{pilA}-*nptII*) with a mini-Tn*5*-Gm^R (encoding gentamycin resistance, Gm^R). Selecting for kanamycin-resistant transposon mutants in which P_{pilA}-*nptII* expression had been restored (Fig. 3a), we isolated one such mutant (*mucR1*::Tn*5*) and determined the Tn*5* insertion to be in the middle (codon 74) of the *mucR*-like gene *CC_0933* (*CCNA_00982*, henceforth *mucR1*; Supplementary Fig. 1D). MucR1 belongs to the conserved MucR/Ros family of transcriptional regulators that harbour a zinc-finger-type fold[24] and control virulence, symbiosis and/or motility in the human pathogen *Brucella suis*[25], the plant pathogen *Agrobacterium tumefaciens*[26] and the plant symbiont *Sinorhizobium fredii* NGR234 (ref. 24).

Unexpectedly, and in contrast to the *mucR1*::Tn*5* allele, an in-frame deletion of *mucR1* (Δ*mucR1*) did not mitigate the defect in P_{sciP}-*lacZ* and P_{pilA}-*lacZ* transcription (Fig. 1c and Supplementary Fig. 2A,B) and PilA expression (Fig. 3b) of Δ*pleC* cells. However, when an in-frame deletion of *mucR1* was introduced along with a deletion in the gene encoding the MucR2-paralog CC_0949 (*CCNA_00998*, henceforth *mucR2*,), the P_{sciP}-*lacZ* and P_{pilA}-*lacZ* activity in the Δ*pleC* Δ*mucR1/2* triple mutant even exceeded that of the Δ*pleC* *mucR1*::Tn*5* cells (Supplementary Fig. 2A,B). By contrast, reporter activity was hardly altered after deletion of either *mucR1* or *mucR2* from Δ*pleC* cells (Supplementary Fig. 2A,B and Table 1).

Trans-dominance of *mucR1*::Tn*5* on *mucR2*. The results above suggest that the *mucR1*::Tn*5* insertion not only disrupts *mucR1* but also causes *trans*-dominance on *mucR2*. Several findings support this conclusion. First, a multi-copy plasmid carrying the coding sequence of truncated MucR1 from *mucR1*::Tn*5* (pMT335-$mucR1^{Tn5}$, see Methods section) alleviates the PilA (Fig. 3b) and P_{pilA}-*lacZ* (Supplementary Fig. 2C) expression defect of Δ*pleC* Δ*mucR1* double-mutant cells, while an analogous plasmid with *WT* *mucR1* (pMT335-*mucR1*) does not. Second, MucR1 and MucR2 directly associate with P_{pilA} and P_{sciP} *in vitro* (as determined by electrophoretic mobility shift assays (EMSA); Supplementary Fig. 2D,E) and *in vivo* (qChIP experiments conducted using polyclonal antibodies to MucR1 or to MucR2; Fig. 3c,d). Third, *mucR1*::Tn*5* impairs binding of MucR2 at P_{pilA} *in vivo* (Fig. 3d) and antibodies to MucR1 no longer precipitate P_{pilA} from chromatin of *mucR1*::Tn*5* cells (Fig. 3c). As immunoblotting revealed that *mucR1*::Tn5 encodes a C-terminally truncated form of MucR1 (Fig. 3e) that does not affect MucR2 steady-state levels (Fig. 3f), we conclude that the *mucR1*::Tn*5* mutation not only removes codons required for DNA binding but also interferes with MucR2 binding to its targets. Finally, and most importantly, pull-down experiments using extracts of Δ*mucR1* cells expressing a MucR1 derivative carrying C-terminal tandem affinity purification (TAP) tag revealed that MucR2 interacts with MucR1-TAP and $MucR1^{Tn5}$-TAP (Fig. 4a).

These findings along with the facts that MucR proteins can dimerize[24,27] and that eukaryotic zinc-finger transcriptional regulators form heterodimers[20,28] suggest that the *trans*-dominance of truncated MucR1 on MucR2 is due to the formation of inactive heterodimers. To map the residues in MucR1 that promote such *trans*-dominance on MucR2, we conducted random mutagenesis of *mucR1* to isolate missense mutants that restore kanamycin resistance to Δ*pleC* *pilA*::P_{pilA}-*nptII* cells, akin to the *mucR1*::Tn*5* mutation. We isolated four *mucR1* alleles encoding different single amino-acid substitutions (R85C, L87P, Y97C or Y97H; Supplementary Fig. 1D; see Methods section) that disrupt one or both of the two conserved α-helices (residues 82-89 and 94-101) in the C-terminal DNA-binding domain of *A. tumefaciens* MucR/Ros determined by nuclear magnetic resonance spectroscopy (NMR)[24]. The residue corresponding to R85 of MucR1 is situated within the DNA recognition helix (helix 1) that along with basic residues in the N-terminal globular domain forms a surface-exposed patch that wraps around DNA and establishes specific base contacts[24], suggesting that loss of this basic residue in MucR1 disturbs DNA

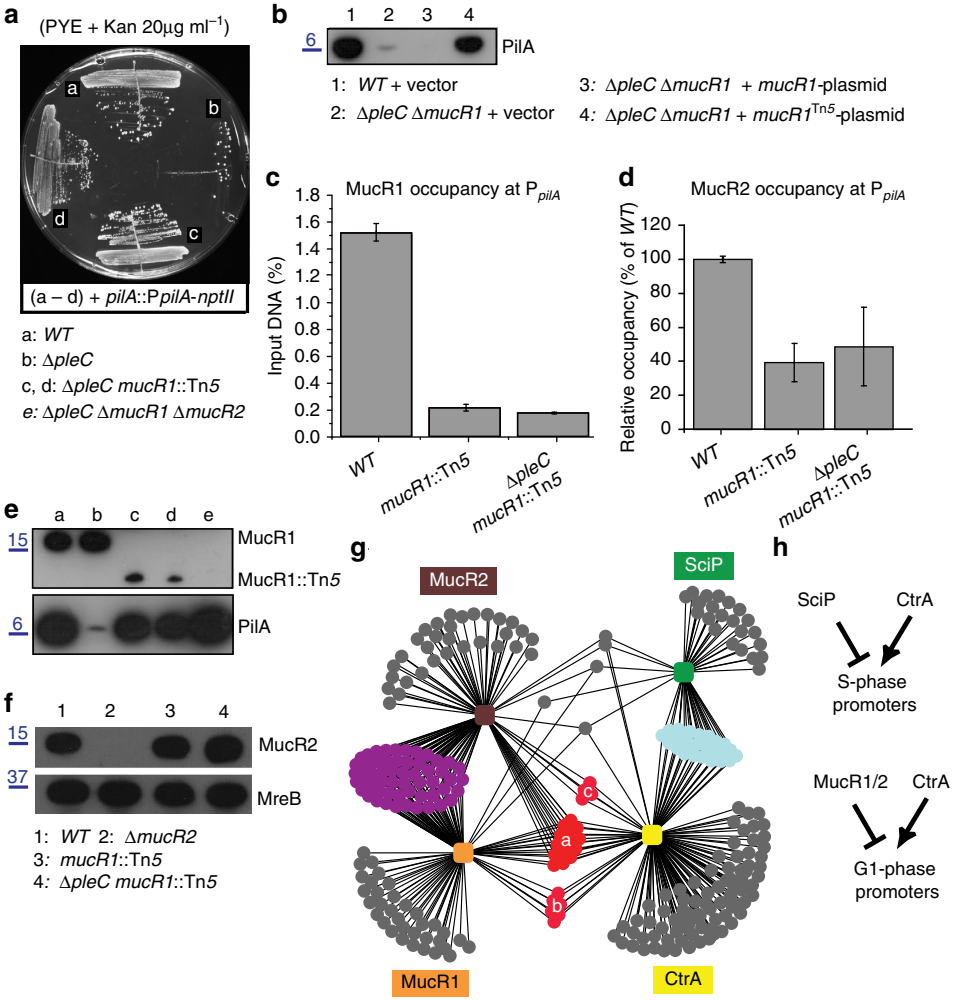

Figure 3 | Identification of *mucR1/2* as negative regulator of PleC:CtrA promoters. (**a**) Growth of *WT* (a) Δ*pleC* (b) and derivatives (c,d) carrying the *pilA*::P_{pilA}-*nptII* transcriptional reporter on PYE plates containing kanamycin (20µg ml^{-1}). (**b**) Immunoblot showing PilA steady-state levels in *WT* and Δ*pleC* Δ*mucR1* double-mutant cells harbouring the empty vector (1 and 2, respectively), and Δ*pleC* Δ*mucR1* cells harbouring either the *mucR1*- (3) or *mucR1*^{Tn5}-plasmid (4). Molecular size standards are indicated on the left as blue lines with the corresponding values (blue) in kDa. (**c**,**d**) Occupancy of MucR1 (**c**) and MucR2 (**d**) at P_{pilA} in *WT*, Δ*pleC mucR1*::Tn*5* double-mutant and *mucR1*::Tn*5* single-mutant cells as determined by qChIP using antibodies to MucR1 or MucR2. Data are from three biological replicates. Error is shown as s.d. (**e**) Immunoblots showing MucR1 and PilA steady-state levels in *WT* (a), Δ*pleC* (b), Δ*pleC mucR1*::Tn*5* double-mutant (c,d) and Δ*pleC* Δ*mucR1* Δ*mucR2* (e) triple-mutant cells. The *mucR1*::Tn*5* allele encodes a truncated derivative of MucR1. Molecular size standards are indicated on the left as blue lines with the corresponding values (blue) in kDa. (**f**) Immunoblots showing MucR2 and MreB (loading control) steady-state levels in *WT* (1), Δ*mucR2* (2), *mucR1*::Tn*5* (3) and Δ*pleC mucR1*::Tn*5* double-mutant (4) cells. Molecular size standards are indicated on the left as blue lines with the corresponding values (blue) in kDa. (**g**) Regulatory network showing putative promoters (dots) bound by CtrA, MucR1, MucR2 and SciP as inferred from ChIP-seq results in *WT* cells (Fig. 2). Common targets between MucR1 and MucR2 are shown in purple, between CtrA and SciP are shown in turquoise and between MucR and CtrA in red. This last group is subdivided into those bound by MucR1/MucR2/CtrA (a), MucR1/CtrA (b) and MucR2/CtrA (c). Note that MucR1/2 and SciP have few common targets. See also Supplementary Data 8 for a prediction of specific and common MucR1 and MucR2 targets. (**h**). Scheme showing the predicted direct regulatory interactions at G1 or late S-phase promoters inferred from **g**.

binding. As pull-down assays showed that MucR1(Y97C)-TAP still interacts with MucR2 (Fig. 4a), we suggest that a MucR1(Y97C) homo-dimer and a MucR1(Y97C)-MucR2 heterodimer are non-functional, and that the other mutations are also loss-of-function mutations that can still interact with MucR2 and thus exert trans-dominance.

Developmental control by MucR1 and MucR2. ChIP-seq analyses with antibodies to MucR1 and to MucR2 predicted 162 and 227 target sites for MucR1 and MucR2 (Fig 2d,e; and Supplementary Data 4 and 5), respectively. Cluster analyses of MucR1/2-, SciP- and CtrA target sites revealed a large overlap between CtrA, MucR1 and MucR2 targets (red set 'a–c', Fig. 3g). Importantly, MucR1 and/or MucR2 bind G1-phase (PleC:CtrA) target promoters *in vivo*, but not SciP targets (Supplementary Data 1, as summarized in Fig. 3h). The occupancy of CtrA and MucR1/2 over four selected promoter regions (including P_{pilA} and P_{sciP}; Fig. 5a–d) revealed overlapping or proximal peaks. Promoter-probe experiments with several of these target promoters confirmed their dependency on MucR1/2 *in vivo* (Table 1).

In support of the notion that MucR1/2 regulates G1-phase promoters, simultaneous deletion of *mucR1* and *mucR2* from *WT* cells (Δ*mucR1/2*) imparts multiple developmental defects, disturbing the acquisition of motility, the buoyancy switch and

Table 1 | Activity of MucR1/2-bound *C. crescentus* promoters in *C. crescentus*.

Strains	*WT*	Δ*R1/R2*	*mucR1*::Tn*5*
Promoters			
perP	100.0 ± 0.0	144.7 ± 17.6	129.8 ± 6.2
CC_0420	102.7 ± 3.5	156.0 ± 14.6	224.6 ± 21.9
CC_0430	107.0 ± 8.3	155.1 ± 4.9	ND ± ND
CC_2810	100.7 ± 3.7	222.1 ± 31.8	206.2 ± 7.0
CC_3001	94.0 ± 7.0	312.2 ± 23.7	186.6 ± 12.2
fljM	93.5 ± 8.0	52.5 ± 4.0	85.8 ± 1.7
CC_2819	100.0 ± 0.7	47.0 ± 2.0	75.8 ± 6.1
flaF	95.6 ± 7.8	86.5 ± 3.1	75.4 ± 3.7
pilA	100.0 ± 0.7	118.7 ± 7.9	119.5 ± 8.9
pilA (synUTR)	100.6 ± 2.7	131.7 ± 2.8	129.2 ± 7.8

Strains	Δ*mucR1*	Δ*mucR2*
Promoters		
CC_0420	120.8 ± 4.1	116.3 ± 2.1
CC_2810	97.3 ± 2.6	129.0 ± 2.9
CC_3001	105.5 ± 3.8	161.5 ± 11.8
CC_2819	94.6 ± 5.1	90.8 ± 4.4
flaF	101.1 ± 1.1	95.9 ± 0.8

ND, not determined; UTR, untranslated region; *WT*, wild-type.
β-Galactosidase activity measurements of extracts from *WT*, *mucR1*::Tn*5*, Δ*mucR1* and Δ*mucR2* single- and double-mutant cells (Δ*R1/R2*) harbouring various *lacZ*-based promoter-probe plasmids. The *pilA(synUTR)*-reporter is a modified version of *pilA* in which the 74 nt UTR has been replaced by a synthetic UTR from *E. coli* (see Supplementary Note 1 for sequence). Error is shown as s.d.

holdfast gene expression (see below). These deficiencies are corrected when Δ*mucR1/2* cells are complemented with a pMT335-derived plasmid harbouring *mucR1* or *mucR2*, but neither by a derivative harbouring *mucR1*^{Tn5} (Fig. 6a,b) nor by the distantly related *mucR*-paralog *CC_1356* (*CCNA_01418*). Moreover, the developmental defects are attenuated by mutations in *ctrA* or *sciP* that suppress the Δ*mucR1/2* motility defect (see motile flare in Fig. 6b and Supplementary Fig. 3A,B; see below).

The *mucR1/2-sciP-ctrA* regulatory module. Promoter-probe and immunoblotting experiments revealed that the activity of flagellar promoters (Supplementary Fig. 3E) and the abundance of class III and class IV flagellar proteins are diminished in Δ*mucR1/2* cells relative to *WT* (Fig 6c,d). Since class II flagellar promoters are bound by SciP (but not MucR1/2, see above) *in vivo* and required for expression of class III and IV flagellar genes[14] and since transcription of *sciP* is negatively regulated by MucR1/2 (Supplementary Fig. 2B), we hypothesized that SciP represses S-phase promoters ectopically in Δ*mucR1*/2 cells (Fig. 6e). Four lines of evidence support this conclusion. First, the promoters that are most efficiently bound by SciP *in vivo* (Supplementary Data 2, including P_{pleA}, P_{flgB}, P_{CC_3676} and P_{CC_3439}) are the most downregulated in Δ*mucR1*/2 cells (Supplementary Figs 3E and 4A). Second, as predicted, CtrA also targets these four promoters (Supplementary Fig. 4) and induces a peak in transcript accumulation in S-phase[16]. Third, suppressor mutations in either *sciP* or *ctrA* augment the activity of these promoters in Δ*mucR1*/2 cells (Supplementary Fig. 4A). Fourth, comparative ChIP-seq of *WT* and Δ*mucR1*/2 cells revealed an increase in abundance of SciP at its preferred target sites in Δ*mucR1*/2 versus *WT* cells (for example, with a $\log_2$ difference of < -0.6 for P_{CC_3676}, P_{CC_3439}, P_{fliQ}, P_{pleA}, and P_{fliX}; Supplementary Data 6). Thus, while the *mucR1/2-sciP-ctrA* module maintains the correct balance in motility gene expression, deletion of *mucR1/2* introduces an imbalance in regulation through SciP.

The eleven suppressor mutations in *sciP* that we isolated are scattered throughout the entire (93-residue) coding region (Supplementary Fig. 3B), suggesting that reduced SciP function (or abundance) can be beneficial in the absence of MucR1/2. Importantly, the T65A mutation lies in a residue previously implicated in SciP function[17], and we observed that derivatives of pMT335 harbouring either *sciP(T24I)* or *sciP(T65A)* are less efficient than the *WT sciP* version in inhibiting motility (of *WT* cells; Supplementary Fig. 3F). The three suppressor mutations that we found in *ctrA* (encoding T168A, T170A and T170P; Supplementary Fig. 3A) all map to the predicted DNA-binding domain. Interestingly, a related mutation (T170I) encoded by the *ctrA401ts* allele[12] impairs motility and prevents growth at 37 °C, while allowing growth at 28 °C. By contrast, *WT* strains harbouring *ctrA(T170A)* in place of *WT ctrA* exhibited no such temperature sensitivity. Thus, unlike the hypomorphic *ctrA401ts* allele, *ctrA(T170A)* acts as a hypermorphic allele. In support of this conclusion, motility is not inhibited upon mild overexpression of SciP from pMT335 in *ctrA(T170A)* cells. By contrast, *ctrA*$^+$ cells harbouring pMT335-*sciP* are non-motile (Fig. 6f; and Supplementary Fig. 3C,D). These findings support the conclusion that transcription of *sciP* in G1-phase prevents activation of motility and other S-phase genes by CtrA (Fig. 6e), and that inappropriate expression of *sciP* from a multi-copy plasmid or by the Δ*mucR1*/2 mutation prevents activation of these promoters in S-phase. Hypomorphic mutations in SciP (for example, T65A) or hypermorphic mutations in the CtrA DNA-binding domain (for example, T170A) mitigate these effects, presumably because the T170A substitution enhances CtrA's ability to compete against repression by SciP *in vivo*.

The Δ*mucR1*/2 mutation also results in a diminished promoter activity (67% reduction versus *WT*) of the *hfsJ* holdfast gene (*CC_0095*)[29] and a buoyancy defect (Fig. 6e). Although the genetic basis of the *Caulobacter* buoyancy has not yet been determined, we found that the Δ*mucR1*/2 buoyancy defect is reversed by the suppressor mutations in *sciP* and *ctrA* (Fig. 6e). Thus, the *mucR1/2-sciP-ctrA* module appears to act on an unknown buoyancy gene(s). Intriguingly, our ChIP-seq experiments revealed that the 26-kb genomic island that is located *circa* 480-kb clockwise from *Cori* and encodes at least one unknown buoyancy determinant[30] harbours the preferred binding sites of MucR1 and target sites of MucR2 (Figs 2d–f; and Supplementary Data 4,5 and 7). To explore this defect further, we conducted a *himar1* transposon (*Tn*) mutagenesis experiment in *mucR1/2* mutant cells and uncovered five buoyancy pseudo-reversion mutants, each harbouring a Tn insertions in the same gene (*CCNA_04006,* encoded on the aforementioned 26-kb genomic island, Fig. 2f) whose predicted translation product resembles the putative N-acetyl-L-fucosamine transferase WbuB from *Escherichia coli*[31]. An in-frame deletion in *CCNA_04006* (Δ*CCNA_04006*) recapitulates the buoyancy pattern of the *Tn* mutation in either Δ*mucR1/2* or *WT* cells (Fig. 2g) and is corrected when CCNA_04006 is expressed from a plasmid (pMT335-*CCNA_04006*), indicating that deletion of *mucR1/2* affects *CCNA_04006*-dependent buoyancy switch.

Direct and positive auto-regulation of *mucR1/2* and *ctrA*. Above we reported the functional and regulatory interactions between *mucR1/2-sciP* and between *mucR1/2-ctrA*. Interestingly, MucR1/2 bind P_{sciP} and the ChIP-seq data traces in Fig. 4b indicate that MucR1 also binds the *ctrA* promoter. This notion was confirmed by EMSAs showing that His_6-SUMO-MucR1, but not His_6-SUMO-MucR2 or His_6-SUMO, binds a *ctrA* promoter probe (Fig. 4d), albeit with somewhat lower affinity than the

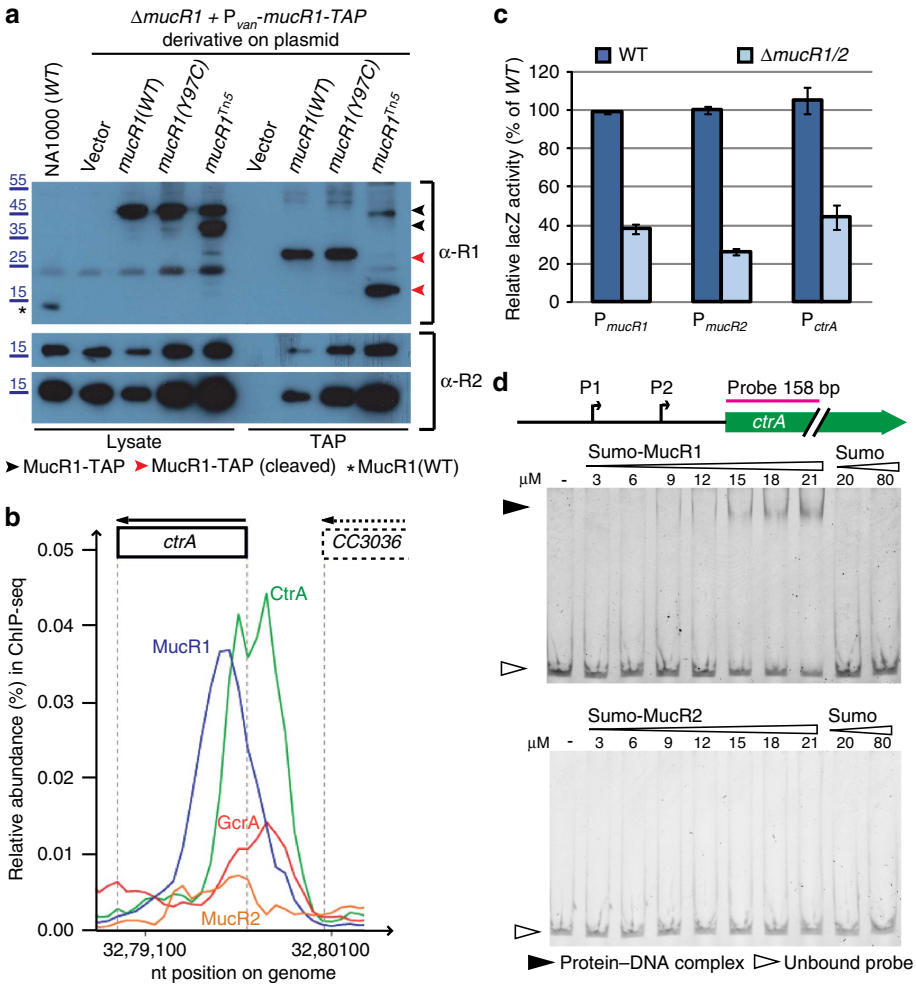

Figure 4 | Heterodimerization and auto-regulation by MucR1/2. (**a**) Immunoblots showing that MucR2 co-purifies with MucR1-TAP before (that is, in cell lysates, lysate) or after the first TAP purification step (cleavage with TEV protease, TAP). The upper panel shows a blot probed with antibodies to MucR1 (α-R1). The asterisk indicates untagged MucR1 in wild-type (NA1000) cells. The arrowheads indicate MucR1-TAP before (black) or after (red) cleavage of the protein-A moiety in the TAP tag with the TEV protease, eluting the proteins from the IgG agarose beads. The two lowest panels shows a blot probed with antibodies to MucR2 (α-R2) revealed at two different exposures. The lower amount of MucR2 that co-purifies with *WT* MucR1-TAP compared with MucR1(Y97C) or MucR1^{Tn5} proteins is likely because of a reduction in the total MucR2 levels when MucR1 is overexpressed. Molecular size standards are indicated on the left as blue lines with the corresponding values (blue) in kDa. (**b**) Traces of the occupancy of various transcription factors at the *ctrA* promoter based on ChIP-seq data. (**c**) β-Galactosidase measurements in extracts of *WT* (dark blue) and Δ*R1/2* (light blue) cells harbouring a P_{ctrA}-, P_{mucR1}- or P_{mucR2}-*lacZ* promoter-probe plasmid. Data are from three biological replicates. Error is shown as s.d. (**d**) Electrophoretic mobility shift assay (EMSA) showing the binding of His$_6$-SUMO-MucR1 or -MucR2 to P_{ctrA}. The white arrows indicate the unbound probe. The black arrows indicate the shifted *ctrA* probes bound by MucR1. His$_6$-SUMO-MucR2 or His$_6$-SUMO does not retard the probe.

P_{pilA} or P_{sciP} probes (Supplementary Fig. 2D,E). Moreover, transcription from a *ctrA* promoter reporter plasmid (P_{ctrA}-*lacZ*) is reduced by 60% in Δ*mucR1/2* cells (Fig. 4c). Thus, MucR can also act positively on its target promoters as observed for other MucR proteins[25,32], and a direct regulatory and functional relationship exists between *mucR* and *ctrA*.

ChIP-seq also indicated a direct auto- and cross-regulatory relationship between MucR1 and MucR2 (Supplementary Data 4 and 5). P_{mucR1}-*lacZ* and P_{mucR2}-*lacZ* promoter-probe reporters are reduced by 62% and 72%, respectively, in Δ*mucR1/2* cells relative to *WT* (Fig. 4c). Although the steady-state levels of MucR1 and MucR2 remain fairly constant during the cell cycle (Supplementary Fig. 5A) and MucR1 occupancy at P_{pilA} in Δ*pleC* cells is near the occupancy seen in *WT* cells, we found that a Tn*5* insertion in the cell cycle kinase genes *divJ* or *divL* (that act in the PleC-signaling pathway[13]) increases the occupancy of MucR1 at P_{pilA} in Δ*pleC* cells (Supplementary Fig. 5B). This *divJ*- or *divL*-dependent increase of MucR binding is not because of diminished CtrA occupancy at P_{pilA}, P_{tacA} or P_{fliL} (Supplementary Fig. 6A–C). Moreover, the recruitment of RNAP to P_{pilA} (Supplementary Fig. 6D) and the production of PilA is restored (Supplementary Fig. 1D in ref. 33). Finally, the abundance of CtrA∼P is not reduced by these mutations in *divJ* and *divL* (Supplementary Fig. 6E). Thus, components of the cell cycle regulatory circuitry such as DivJ and DivL can modulate the occupancy of MucR1 on its targets. Conversely, MucR1 directly regulates expression of the master cell cycle regulator CtrA.

Taken together, we conclude that *mucR*1/2 is a critical component of an integrated and homeostatic (auto)regulatory module, *mucR1/2-ctrA-sciP*, in which MucR not only engages in a double-negative regulation (MucR and SciP), but also in a double-positive one (MucR and CtrA) that likely helps reinforce and/or synchronize the molecular events underlying the S→G1 transcriptional switch.

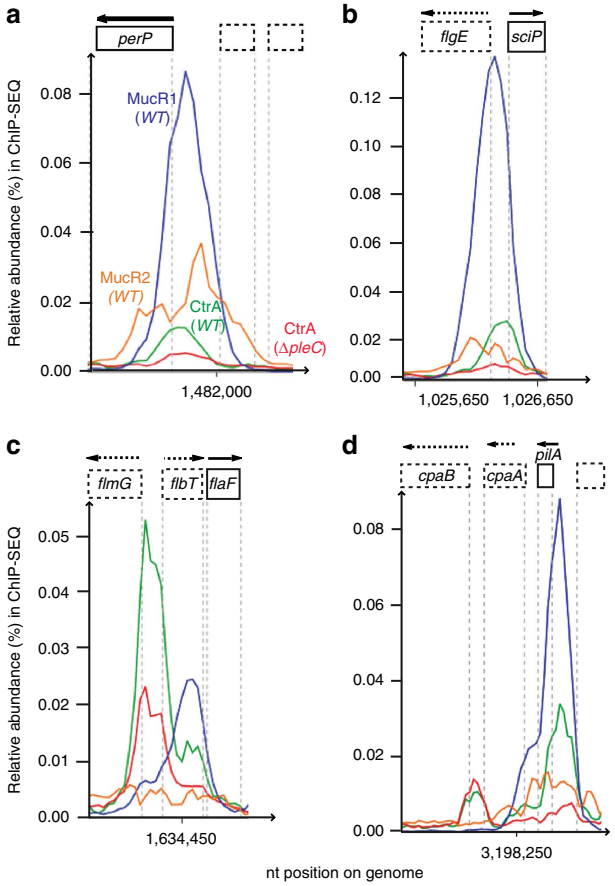

Figure 5 | PleC:CtrA target promoters that are bound and regulated by MucR1/2. (**a**–**d**) Traces of the occupancy of MucR1 (blue), MucR2 (orange) and CtrA (green) in *WT* cells and CtrA in Δ*pleC* (red) cells as determined by ChIP-seq data. Note that in panel **c**, the MucR1 binding overlaps the second binding site of CtrA upstream of the *flaF* gene.

Pan-genomic ChIP-seq reveals conserved target regulation. To investigate whether the link of MucR with the cell cycle circuitry has been maintained during evolution, we first assessed the extent of the functional conservation in the symbiont *S. fredii* NGR234 (henceforth *S. fredii*) that also contains two *mucR*-like genes: *a00320* on the symbiotic plasmid pNGR234a and *c07580* on the chromosome. Both *a00320* and *c07580* can substitute for *Caulobacter mucR1/2* in motility control (Fig. 7a), as is also the case for the unique *mucR* homologues encoded in the genomes of the animal pathogen *B. suis* and the plant pathogen *A. tumefaciens* (Fig. 7a), indicating that expression of *sciP* and the downstream motility target genes are sufficiently controlled by the heterologous MucR proteins to support motility. Because of this functional conservation, we asked if direct regulatory interactions were also maintained. To this end, we conducted pan-genomic ChIP-seq analyses using the antibodies to *Caulobacter* MucR1 and MucR2 to identify promoters bound by MucR-like proteins in *S. fredii* (Fig. 7b; Supplementary Fig. 7A; and Supplementary Data 4 and 5). We then used these promoters to show the converse genetic dependency, that is, that these MucR-bound *S. fredii* promoters are regulated by *Caulobacter mucR1/2*. Indeed, promoter-probe experiments with *Caulobacter WT* and Δ*mucR1/2* cells revealed that six *S. fredii* promoters are regulated negatively and two positively by MucR1/2 (out of 10 promoters tested; Table 2).

Next, we attempted to compute pan-genomic consensus motif for MucR from the top 50 MucR1 target sites of *Caulobacter* and *S. fredii* (Fig. 7c) using the MEME algorithm (see Methods section). As proof-of-principle, we also computed a pan-genomic consensus motif of the top 50 CtrA-bound sites in the *Caulobacter* and *S. fredii* genomes determined by ChIP-seq using antibodies to *Caulobacter* CtrA (Supplementary Data 7). The deduced motif is remarkably similar to the CtrA target sequence determined biochemically for *Caulobacter* (TTAA-N7-TTAA; Fig. 7c), showing that this strategy can accurately predict consensus motifs. The pan-genomic consensus motif that was deduced for MucR1 is fairly degenerate, revealing a preference for AT-rich DNA substrates in GC-rich genomes (65% for *Caulobacter* and 61% for *S. fredii*). Indeed, synthetic reporters (T5_*mucR1*b-*lacZ* and two attenuated derivatives; Supplementary Note 1) in which two MucR1 motifs were placed in tandem, downstream of a heterologous strong promoter from *E. coli* T5 phage driving *lacZ* expression are MucR-dependent in *Caulobacter* (Supplementary Fig. 8A,B), thereby validating our predicted pan-genomic MucR1-consensus sequence as a MucR1 target.

Finally, we compared the target sites of CtrA and MucR in *S. fredii* using the consensus sequences. This revealed a suite of overlapping (or proximal) targets as for *Caulobacter*, albeit fewer in number (Fig. 7b). Importantly, several of these target sites in *S. fredii* are linked to orthologous genes that we determined to be under MucR and CtrA control in *Caulobacter* (including *flaF*- and *sciP*-like genes that are cell cycle-regulated and perform developmental functions in *Caulobacter*; Fig. 7d)[4,34]. Thus, the functional and direct regulatory relationships between MucR proteins and the cell cycle are (at least partly) conserved during evolution.

Discussion

Through forward genetics and (pan)genomic promoter occupancy of key cell cycle transcriptional regulators, we unearthed a conserved regulatory module, *mucR1/2-sciP-ctrA*, that implements the S→G1 switch in *Caulobacter*. The ancestral zinc-finger transcription factor paralogs MucR1/2 repress G1-phase promoters that are activated by the essential master regulator CtrA including that controlling the negative regulator SciP that turns off S-phase promoters activated by CtrA. Through this double-negative wiring, the induction of G1-promoters occurs concomitantly with the repression of S-phase promoters. Superimposed on this double-negative regulatory wiring is a double-positive circuit in which MucR1/2 promotes expression of CtrA. Thus, MucR has both negative and positive roles in reinforcing the S→G1 transcriptional switch in *Caulobacter*.

Remarkably, G1-phase-specific transcripts were recently also detected in synchronized *S. meliloti*[5], raising the intriguing possibility that the underlying regulatory mechanisms that direct G1-phase transcription in *Caulobacter* also operate in symbiotic or virulent relatives, and that the *mucR-sciP-ctrA* regulatory module coordinates virulence/symbiosis and cell cycle transcription. Several findings are consistent with this notion. First, MucR proteins were previously described as regulators of virulence and symbiosis gene expression in *Brucella*, *Sinorhizobia* and *Agrobacteria* that also divide asymmetrically[3,25,35]. Second, we showed that MucR1/2 are required for proper implementation of the cell cycle transcriptional programs in dividing *Caulobacter* cells. Third, we found that MucR from *Brucella*, *Sinorhizobia* and *Agrobacteria* can confer motility to *Caulobacter* Δ*mucR1/2* mutants, a function that is dependent on proper cell cycle-dependent expression of SciP in G1-phase, while mis-expression of SciP impairs motility gene expression and leads to non-motile cells in soft agar (Fig 6b,f). Fourth, MucR-bound promoters of *S. fredii NGR234* are also under MucR1/2 control in *Caulobacter*

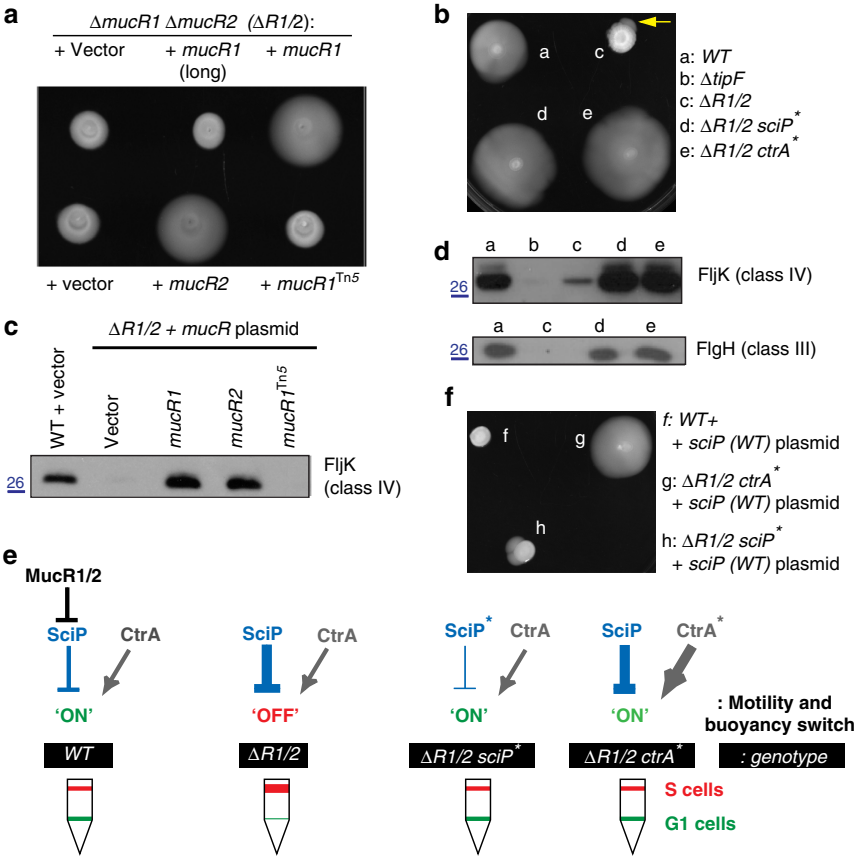

Figure 6 | Regulatory interplay between *mucR1/2*, *sciP* and *ctrA* in the control of motility. (**a**,**b**). The motility defect of Δ*mucR1* Δ*mucR2* double-mutant cells (Δ*R1/2*) can be rescued by expression of *mucR1* or *mucR2* from a plasmid or by point mutation in *sciP* or *ctrA*. (**a**) Motility plates (0.3% agar) inoculated with Δ*R1/2* cells containing the empty plasmid or derivatives with *mucR1* (long form, original annotation of *CC_0933*), *mucR1*^{Tn5} or the plasmids carrying *mucR1* (*CCNA_00982*) or *mucR2* (*CCNA_00998*). (**b**) The motility of Δ*R1/2* (c) cells harbouring point mutation in *sciP* (d) or in *ctrA* (e) relative to *WT* cells (a). The yellow arrow points to the emergence of motile suppressors from a non-motile inoculum of Δ*R1/2* cells (c) versus *WT* (a) cells on motility agar. (**c**) Immunoblot showing the abundance of a class IV gene product (the FljK flagellin) in the supernatant of *WT* and Δ*R1/2* cells containing the plasmids described in **a**. Molecular size standards are indicated on the left as blue lines with the corresponding values (blue) in kDa. (**d**) Immunoblots showing the steady-state levels of a class IV gene product (the FljK flagellin) and a class III gene product (the FlgH L-ring protein) in *WT* (a), Δ*R1/2* (c), Δ*R1/2 sciP** (d) and Δ*R1/2-ctrA** (e) cells. Also shown are the FljK levels in Δ*tipF* cells as a comparison (b). Molecular size standards are indicated on the left as blue lines with the corresponding values (blue) in kDa. (**e**) Model based on the regulatory interactions elucidated above. Misregulation of *sciP* expression in Δ*R1/2* impairs motility. A hypomorphic allele of *sciP* (*sciP**) or hypermorphic allele of *ctrA* (*ctrA**) can restore motility to Δ*R1/2* cells. The buoyancy phenotype in *WT* and mutant cells is shown underneath. Note that the *sciP** and *ctrA** mutations restore the *WT* buoyancy phenotype, indicating adequate regulation of buoyancy effector(s). (**f**) The *sciP* overexpression plasmid pMT335-*sciP* inhibits motility in the *WT* (f) and in Δ*R1/2 sciP** (h), but not Δ*R1/2 ctrA** (g) cells.

(Table 2). Finally, our pan-genomic-binding site studies in *Caulobacter* and in the symbiont *S. fredii* revealed that many orthologous genes carry binding sites for MucR and CtrA in both species (Fig. 7d). With this close interplay of cell cycle transcription and virulence/symbiotic functions in mind, it is tempting to propose that certain transcriptional regulators previously thought to function exclusively as regulators of virulence/symbiosis should be re-classified as regulators of cell cycle transcription that restrict virulence gene expression to a specific cell cycle stage. For example, MucR proteins could endow a G1-phase-arrested daughter cell in *Brucella*, *Sinorhizobia*, *Agrobacteria* and likely other Alpha-proteobacteria with the necessary transcripts to establish virulence or symbiosis in the host. Indeed, motility and cell envelope-associated polysaccharides (responsible for the *muc*oid colony morphology) are both critical for virulence and known to be MucR controlled in *Sinorhizobia* and *Brucella*[3,25,35].

Interestingly, the fact that heterologous MucR proteins control cell cycle transcription indicates that they are properly regulated in *Caulobacter*, implying that MucR control is conserved in the Alpha-proteobacteria[6]. MucR1/2 protein levels remain relatively constant during the *Caulobacter* cell cycle, suggesting that MucR is regulated post-translationally. Indeed, the ability of heterologous MucR proteins to support function in another host is easier to reconcile with regulation by a small molecule that is produced by most Alpha-proteobacteria, rather than by a very promiscuous factor that must recognize the different MucR proteins.

Several Alpha-proteobacteria including *Caulobacter* and *S. fredii* encode multiple MucR paralogs, and we show that the *Caulobacter* MucR paralogs can heterodimerize akin to eukaryotic zinc-finger transcription factors[28]. Although a single endogenous or a heterologous MucR paralog can support cell cycle transcription in *Caulobacter*, it is conceivable that heterodimerization serves to fine-tune MucR activity and cell cycle transcription. With the eukaryotic mitochondrion having descended from an Alpha-proteobacterium[21] and ancestral zinc-finger transcription factors being primarily represented in the

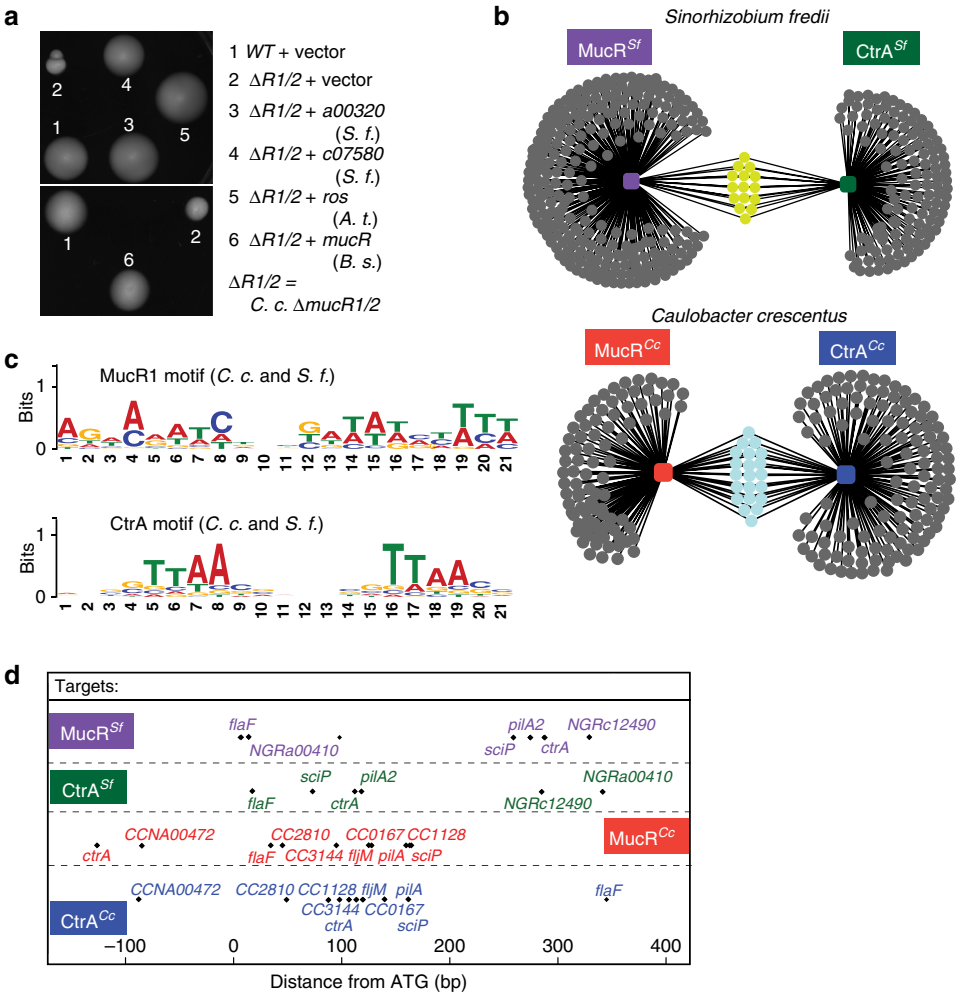

Figure 7 | Conservation of direct regulation by MucR and CtrA in *C. crescentus* and *S. fredii* NGR234. (**a**) Motility agar was inoculated with *WT* and *ΔR1/2* containing the empty vector or derivatives with *mucR* homologues from different alpha-Proteobacteria: *S. fredii (S. f) a00320* (3) and *S. f c07580* (4), *A. tumefaciens* (*A. t*) *ros* (5), *B. suis* (*B. s*) *mucR* (6). (**b**) Network of DNA targets shared by CtrA and MucR in *S. fredii* str. NGR234 (*S. f.*, upper) and in *C. crescentus* (*C. c.*, lower). (**c**) *In silico* deduced binding motif of CtrA and MucR for *C. c.* and *S. f.* (**d**) Relative distance of CtrA- and MucR1-binding site relative to the ATG of common targets in *C. c.* and in *S. f. NGR_c12490* is orthologous to *CC_0167* and *NGR_a00410* to *CCNA_00472*.

Table 2 | Activity of MucR-bound *S. fredii* promoters in *C. crescentus*.

Strains	*WT*	*ΔR1/2*
Promoters		
NGRa00570	96.0 ± 7.0	151.1 ± 9.4
NGRa00610	100.0 ± 1.2	205.6 ± 16.7
NGRa02310	101.4 ± 3.0	150.9 ± 4.9
NGRa03530	100.1 ± 1.8	462.4 ± 27.4
NGRc06240	99.8 ± 2.6	387.5 ± 34.8
NGRc28620	98.1 ± 3.4	238.1 ± 24.5
NGRc35630	100.1 ± 3.0	63.5 ± 4.0
NGRc11500	100.0 ± 0.3	23.5 ± 1.3

β-Galactosidase activity measurements of extracts from *WT* and *ΔmucR1 ΔmucR2* double-mutant cells (*ΔR1/R2*) harbouring various *lacZ*-based promoter-probe plasmids with *S. fredii* promoters thought to be bound by *S. fredii* MucR based on the ChIP-seq data shown in Supplementary Data 4 and 5. Error is shown as s.d.

Alpha-proteobacterial lineages, it is conceivable that these transcription factors originated in an Alpha-proteobacterium that had undergone a duplication of the *mucR* gene.

Methods

Strains and growth conditions. *Caulobacter* NA1000 (ref. 10) and derivatives were grown at 30 °C in PYE (peptone–yeast extract) or M2G (minimal glucose). *S. fredii* NGR234 (ref. 36) was grown at 30 °C in tryptone–yeast extract. *E. coli* S17-1 *λpir*[37] and EC100D (Epicentre Technologies, Madison, WI) were grown at 37 °C in Luria broth. The *E. coli* mutator strain XL1 Red (Agilent Technologies Inc., Cedar Creek, TX) was grown at 30 °C in Luria broth. Motility assays, swarmer cell isolation, electroporations, biparental matings and bacteriophage ΦCr-30-mediated generalized transductions were performed as described[33,38–40].

Identification of *mucR1*. The *mucR1*::Tn*5* insertion was identified using a modification of the kanamycin resistance suppressor screen[33]. In brief, we screened for mini-Tn5 insertions that restore P*pilA* firing to Δ*pleC* cells bearing P_{pilA}-*nptII* transcriptional reporter that confers kanamycin resistance to 20 μg ml^{-1} when P*pilA* is fully active. In contrast to previous screens that were done using a mini-Tn5 conferring resistance to tetracycline, in this screen a version was used that confers resistance to gentamycin. The delivery plasmids pSS88 and pSS87 (ref. 41) were used to mutagenize Δ*pleC pilA*:: P_{pilA}-*nptII* cells by biparental mating with the mini-Tn*5*, screening for colonies that were resistant to gentamycin (1 μg ml^{-1}), kanamycin (20 μg ml^{-1}) and nalidixic acid (20 μg ml^{-1}, nalidixic acid is used to counter-select against the *E. coli* donor in biparental matings). This mutagenesis screen gave rise to one isolate (NR513) with the desired resistance profile. The Tn*5* insertion in NR513 was mapped to the uncharacterized *CC_0933* gene at nucleotide (nt) position 1061847 of the *C. crescentus* NA1000 genome sequence (Supplementary Fig. 1C) using arbitrarily primed PCR[33].

Strain constructions. The Δ*mucR1* and Δ*mucR2* marker-less single and double deletions were introduced into *WT* (NA1000) and Δ*pleC*[42]cells using the standard two-step recombination sucrose counter-selection procedure induced by the pNPTS138 derivatives. The resulting strains are the Δ*mucR1* and Δ*mucR2* single mutants, the Δ*pleC* Δ*mucR1*, Δ*pleC* Δ*mucR2* and Δ*mucR1* Δ*mucR2* double mutants, and the Δ*pleC* Δ*mucR1* Δ*mucR2* triple mutant. Deletions were confirmed by PCR using outside primers that do not hybridize within the *mucR* deletion alleles carried on pNPTS138.

The *mucR1*::Tn*5* mutation (conferring gentamycin resistance and encoding a truncated MucR1 derivative that is dominant negative on MucR2) was transduced from strain NR513 (see below) into the *WT* (NA1000) and Δ*pleC* strains by ϕCr30-mediated generalized transduction, yielding strains in which endogenous *mucR1* is replaced by *mucR1*::Tn*5*.

The P-*lacZ* transcriptional reporter strains were made by electroporation of the different plac290-based transcriptional reporter plasmids into *WT* (NA1000), Δ*pleC*, Δ*mucR1* Δ*mucR2*, Δ*pleC* Δ*mucR1* Δ*mucR2*, and the motile Δ*mucR1* Δ*mucR2* second-site suppressor mutants UG1277 (Δ*mucR1* Δ*mucR2* $sciP^{T24I}$) and UG1280 (Δ*mucR1* Δ*mucR2* $ctrA^{T170A}$).

The *pleC*::Tn*5* derivatives shown in Fig. 1f were made by generalized transduction of from SC1035 (ref. 43) into NA1000 or Δ*ctrA*:: Ω cells harbouring pSAL14 or pCTD14 (ref. 44).

Isolation of phosphomimetic variants of *ctrA*, $ctrA^{gof}$. We identified $ctrA^{gof}$ alleles (gain of function, gof) by virtue of their ability to allow growth as sole copy of *ctrA* in a strain lacking the gene encoding the hybrid histidine kinase/phosphatase CckA (*cckA*) gene. To this end, the pMT464-ctrA plasmid was passaged through the *E. coli* mutator strain XL1 Red. The mutant library was subsequently electroporated into the Δ*cckA*::Gent; *ctrA*::Spc double-mutant strain carrying pCTD14 (pJS14-*ctrAD51E* conferring resistance to chloramphenicol)[45] and colonies that grew in the presence of kanamycin (20 μg ml^{-1}) and 0.3% xylose were selected, as they were candidates in which pCTD14 had been displaced by a mutant pMT464-*ctrA* plasmid that can support growth in the absence of CckA (note that pCTD14 and pMT464 have the same origin of replication). The new $ctrA^{gof}$ alleles were sequenced, excised by cleavage with *Nde*I and *Eco*RI and cloned into pMT335 for further analysis in strains carrying the plac290-based P_{pilA}-*lacZ* reporter plasmid. The mutant variants identified code for D8G, D8N, D51E, N53D or M99I. Note that the isolation of D51E, a known phosphomimetic allele[44], validates the screen.

Isolation of missense mutations in *mucR1*. To isolate missense mutations in *mucR1* that phenocopy the *mucR1*::Tn*5* mutation, plasmid pMT375-*mucR1* was mutated by passage through *E. coli* XL1 Red mutator strain (Agilent Technologies) on ampicillin. The mutagenized plasmid library was then electroporated into Δ*pleC* Δ*mucR1*; P_{pilA}-*nptII* cells, selecting for resistance to tetracycline (1 μg ml^{-1}) and kanamycin (20 μg ml^{-1}). The new loss-of-function mutations that phenocopy the effect of *mucR1*::Tn*5* were excised by restriction with *Nde*I and *Eco*RI and cloned on pMT335 to assess their effects in strains carrying the plac290-based P_{pilA}-*lacZ* promoter-probe plasmid.

Motility suppressors of Δ*mucR1* Δ*mucR2* double-mutant cells. Spontaneous mutations that suppress the motility defect of the Δ*mucR1* Δ*mucR2* double mutant appeared as 'flares' that emanated from the non-motile colony after approximately 4–5 days of incubation. After isolating 14 motile Δ*mucR1*/2 suppressor mutants, two isolates (UG1277 and UG1278) were subjected to whole-genome sequencing and mutations in the *sciP* gene ($sciP^{T24I}$ and $sciP^{T65A}$, respectively) were found. In UG1277, the threonine codon (ACT) at position 24 in *sciP* is changed to one encoding isoleucine (ATT). In UG1278, the threonine codon (ACG) at position 65 in *sciP* is changed to one encoding alanine (GCG). Since SciP has been implicated in the regulation of CtrA, we sequenced *sciP* and *ctrA* in other suppressor mutants and found a mutation in strain UG1280 ($ctrA^{T170A}$) in which the codon of threonine (ACC) at residue 170 was exchanged for one encoding alanine (GCC). To confirm that the mutations $sciP^{T24I}$ and $ctrA^{T170A}$ were responsible for the suppression of motility defect of the Δ*mucR1* Δ*mucR2* double mutant, we backcrossed each of the mutations into the Δ*mucR1* Δ*mucR2* strain. To this end, a pNPTS138 derivative (pNPTS138-hook, conferring kanamycin resistance) was integrated by homologous recombination nearby the *sciP* locus in UG1277. Next, ΦCr-30-mediated generalized transduction was used to transfer the mutant *sciP* allele from UG1277 into the Δ*mucR1* Δ*mucR2* mutant. Finally, the sucrose counter-selection procedure (see above) was used to select for stains that had lost pNPTS138-hook by homologous recombination. To backcross $ctrA^{T170A}$ from UG1280 into Δ*mucR1* Δ*mucR2* strain and the *WT* (NA1000) parent, the pNPTS138 derivative (pNPTS138-*ctrA-ds*) was integrated nearby the *ctrA* locus of UG1280 by homologous recombination. ΦCr-30-mediated generalized transduction was used to transfer the mutant *ctrA* allele from UG1280 into the recipients by selecting for kanamycin resistance. Clones that have lost pNPTS138-*ctrA-ds* by homologous recombination were probed for kanamycin resistance (on PYE plates supplemented with kanamycin) and motility (on swarm agar plates) following sucrose counter-selection. PCR and sequencing was used to verify the integrity of the three mutants in each backcrossing experiment.

Isolation of transposon insertions in *CCNA_04006*. Transposon (*himar1*) mutagenesis of the Δ*mucR1* Δ*mucR2* strain was done using an *E. coli* λ*pir* donor harbouring pHPV414 as described[46]. The mutant library was grown in PYE and then subjected to Percoll density gradient centrifugation, followed by enrichment for cells where the dense swarmer cells band is normally found. After repeated cycles of enrichment (growth in PYE followed by Percoll density gradient centrifugation), the band containing dense cells was extracted and single colonies were isolated on PYE plates. The transposon insertion sites in five clones were mapped as described[46] to nt 475241, 475633, 475659, 475789 and 476186 of the NA1000 genome sequence.

Protein purification and antibody production. For antibody production, His_6-MucR1 or His6-SUMO-SciP(T24I) was expressed from pCWR350 and pUG97 in *E. coli* Rosetta (DE3)/pLysS (EMD Millipore, Billerica, MA), respectively, and purified the recombinant proteins purified under standard native conditions using Ni^{2+} chelate chromatography. They were used to immunize New Zealand white rabbits (Josman LLC, Napa, CA). His_6-SUMO-MucR2 was expressed from pUG12 in *E. coli* Rosetta (DE3)/pLysS and purified using Ni^{2+} chelate chromatography in phosphate-buffered 8 M urea (Qiagen, Hilden, Germany). The protein was excised from a 15 % SDS polyacrylamide gel and used to immunize rabbits.

For EMSAs, soluble His_6-SUMO-MucR1, His_6-SUMO-MucR2 or His_6-SUMO was purified from *E. coli* Rosetta (DE3)/pLysS containing pUG30, pUG41 or pET28a-His_6-SUMO, respectively, under native conditions using Ni^{2+} chelate chromatography. In brief, cells were pelleted, resuspended in lysis buffer (20 mM Tris, 500 mM NaCl, 2 mM $MgCl_2$, 50 mM L-glutamic acid, 50 mM L-arginine and 10 mM imidazole; pH 8.8) and lysed by three passages through a French pressure cell at 20,000 PSI. After centrifugation at 100,000*g* the supernatant was loaded onto a 1 ml HisTrap column (GE Healthcare, Fairfield, CT) and eluted with a linear gradient using the same buffer containing 500 mM imidazole.

Electrophoretic mobility shift assays. His_6-SUMO-MucR1, His_6-SUMO-MucR2 or His_6-SUMO were always freshly diluted into the binding buffer (25 mM Tris, 100 mM KCl, 5 mM MgCl2, 5 % glycerol and 0.05 % dodecyl maltoside, pH 7.5) to test the binding to the different Cy3-labelled DNA fragments. They were mixed with BSA (0.5 mg ml^{-1} BSA), sonicated salmon sperm DNA (0.05 mg ml^{-1}, Invitrogen Carlsbad, CA) and the Cy3-labelled DNA fragments (25 nM) in a total volume of 15 μl. The samples were incubated at room temperature for 10 min, then 5 μl 4 × loading dye (4 × binding buffer in 40% glycerol) was added, the samples separated on a 4% TBE polyacrylamide gel and the gel was scanned with a Typhoon FLA 7000 imager (GE Healthcare). Gel-purified 5′ Cy3-labelled PCR fragments (Macherey-Nagel, Bethlehem, PA) were used as probes.

qChIP assays. Mid-log phase cells were cross-linked in 10 mM sodium phosphate (pH 7.6) and 1% formaldehyde at room temperature for 10 min and on ice for 30 min thereafter, washed three times in phosphate-buffered saline (PBS) and lysed in a Ready-Lyse lysozyme solution (Epicentre Technologies) according to the manufacturer's instructions. Lysates were sonicated (Sonifier Cell Disruptor B-30, Branson Sonic Power Co., Danbury, CT) on ice using 10 bursts of 20 s at output level 4.5 to shear DNA fragments to an average length of 0.3–0.5 kbp and cleared by centrifugation at 14,000 r.p.m. for 2 min at 4 °C. Lysates were normalized by protein content, diluted to 1 ml using ChIP buffer (0.01% SDS, 1.1% Triton X-100, 1.2 mM EDTA, 16.7 mM Tris-HCl (pH 8.1), 167 mM NaCl plus protease inhibitors (Roche, Switzerland) and pre-cleared with 80 μl of protein-A agarose (Roche) and 100 μg BSA. Ten percent of the supernatant was removed and used as total chromatin input DNA as described before[47].

Two microliters of polyclonal antibodies to CtrA[44], SciP[17,18] (note that for ChIP experiments reported in Supplementary Data 6, we used antibodies that we raised against His6-SUMO-SciP), FlbD[48], RpoC (Neoclone, Madison, WI), MucR1 or MucR2 were added to the remains of the supernatant, incubated overnight at 4 °C with 80 μl of protein-A agarose beads pre-saturated with BSA, washed once with low salt buffer (0.1% SDS, 1% Triton X-100, 2 mM EDTA, 20 mM Tris-HCl (pH 8.1) and 150 mM NaCl), high salt buffer (0.1% SDS, 1% Triton X-100, 2 mM EDTA, 20 mM Tris-HCl (pH 8.1) and 500 mM NaCl) and LiCl buffer (0.25 M LiCl, 1% NP-40, 1% sodium deoxycholate, 1 mM EDTA and 10 mM Tris-HCl (pH 8.1)), and twice with TE buffer (10 mM Tris-HCl (pH 8.1) and 1 mM EDTA). The protein DNA complexes were eluted in 500 μl freshly prepared elution buffer (1% SDS and 0.1 M NaHCO3), supplemented with NaCl to a final concentration of 300 mM and incubated overnight at 65 °C to reverse the crosslinks. The samples were treated with 2 μg of Proteinase K for 2 h at 45 °C in 40 mM EDTA and 40 mM Tris-HCl (pH 6.5). DNA was extracted using phenol:chloroform:isoamyl alcohol (25:24:1), ethanol precipitated using 20 μg of glycogen as carrier and resuspended in 100 μl of water. For deep sequencing (ChIP-seq), total chromatin input DNA was not saved. To determine the specificity of MucR antibodies, samples were prepared and treated as for the ChIP, but after the washing steps the beads were resuspended in SDS loading buffer and boiled. Data are from three biological replicates.

Pull-down of MucR2 with MucR1-TAP. Overnight cultures were used to inoculate 80 ml of PYE (containing 50 μM vanillate to induce expression of MucR1-TAP

proteins) and cells were grown to an OD_{600} of 0.5–0.6. Sodium phosphate (pH 7.6) and formaldehyde were added to the cultures to a final concentration of 10 μM and 1%, respectively, and the cells were incubated for 10 min at room temperature followed by 30 min on ice. Cells were harvested by centrifugation (6500 rpm, 10 min at 4 °C) and washed twice in PBS. Cell pellets were resuspended in 900 μl of resuspension buffer (50 mM sodium phosphate, pH 7.4, 1 mM EDTA, 50 mM NaCl, 10 mM $MgCl_2$, 0.5% n-Dodecyl-β-D-maltoside, 1 × protease inhibitors (Complete™ EDTA-free, Roche)) and lysed at room temperature for 15 min with a Ready-Lyse lysozyme solution (Epicentre Technologies). Cell lysates were sonicated (Bioruptor Pico, Diagenode) at 4 °C using 10 cycles of 30 s and cleared by centrifugation at a relative centrifugal force (r.c.f.) of 18,188*g* for 2 min at 4 °C. The supernatant was incubated with IgG Sepharose beads (GE Healthcare Bio-Sciences, Sweden) for 2 h 30 min at 4 °C, washed six times with IPP150 buffer (10 mM Tris-HCl pH 8, 150 mM NaCl and 0.1% NP-40) and four times with TEV buffer (IPP150 buffer plus 0.5 mM EDTA and 1 mM DTT), and incubated overnight at 4 °C with TEV buffer containing 100 U ProTEV Plus protease (Promega) to release the tagged complex. The eluate was used for SDS-PAGE and immunoblotting.

Real-time PCR. Real-time PCR was performed using a Step-One Real-Time PCR system (Applied Biosystems, Foster City, CA) using 5% of each ChIP sample (5 μl), 12.5 μl of SYBR green PCR master mix (Quanta Biosciences, Gaithersburg, MD), 0.5 μl of primers (10 μM) and 6.5 μl of water per reaction. Standard curve generated from the cycle threshold (C_t) value of the serially diluted chromatin input was used to calculate the percentage input value of each sample. Average values are from triplicate measurements done per culture. The final data was generated from three independent cultures. The DNA regions analysed by real-time PCR were from nucleotide −287 to −91 relative to the start codon of *pilA*, −313 to +32 of *fliL*, −226 to +30 of *tacA* and −191 to +14 of *sciP*.

EMSA probe preparation. The different promoter regions were amplified in a PCR using plasmids pJS70 (plac290-based P*pilA-lacZ* transcriptional fusion), pCC_0903-lac290 (*sciP*) or chromosomal DNA of NA1000 (*ctrA*) as templates and with 5′-Cy3-labelled oligonucleotides pilACy3fw and pilACy3rev, sciPCy3fw and sciPCy3rev, ctrACy3fwshort and ctrACy3revshort, or CtrACy3fwlong and CtrACy3revlong (see Supplementary Table 1 for sequences of oligonucleotides). The 5′-Cy3-labelled PCR fragments were gel purified (Macherey-Nagel).

β-Galactosidase assays. β-Galactosidase assays were performed at 30 °C as described earlier[40]. Fifty microlitres of cells at OD_{660nm} = 0.1–0.6 were lysed with chloroform and mixed with 750 μl of Z buffer (60 mM Na_2HPO_4, 40 mM NaH_2PO_4, 10 mM KCl and 1 mM $MgSO_4$ heptahydrate). A quantity of 200 μl of ONPG (4 mg ml^{-1} o-nitrophenyl-β-D-galactopyranoside in 0.1 M KPO_4 pH 7.0) were added and the reaction timed. When a medium-yellow colour was developed, the reaction was stopped with 400 μl of 1 M Na_2CO_3. The OD_{420nm} of the supernatant was determined and the units were calculated with the equation: $U = (OD_{420nm} \times 1{,}000)/(OD_{660nm} \times \text{time (in min)} \times \text{volume of culture (in ml)})$. The assays were done in triplicates and normalization was done by conversion of the Miller Units (absolute values) of one arbitrarily chosen *WT* construct or *WT* background as reference, set to 100%. All absolute values were then converted to relative values, averaged and the error was determined by calculation of the s.d. Data are from three biological replicates.

Antibodies used for immunoblotting and ChIP. Polyvinylidenfluoride membranes (Merck Millipore Headquarters, Billerica, MA) were blocked with PBS, 0.05% Tween 20 and 5% dry milk for 1 h and then incubated for 1 h with the primary antibodies diluted in PBS, 0.05% Tween 20 and 5% dry milk. The different antisera were used at the following dilutions: anti-MucR1 (1:10,000), anti-MucR2 (1:10,000), anti-CtrA (1:10,000)[44], anti-PilA (1:5,000)[49], anti-FlgH (1:10,000)[50], anti-MreB (1:10,000)[51], anti-FljK (1:50,000)[52]. The membranes were washed four times for 5 min in PBS and incubated 1 h with the secondary antibody diluted in PBS, 0.05% Tween 20 and 5% dry milk. The membranes were finally washed again four times for 5 min in PBS and revealed with Immobilon Western Blotting Chemoluminescence HRP substrate (Merck Millipore Headquarters). Antibodies used for ChIP are to CtrA[44], SciP[17,18], FlbD[48], RpoC (Neoclone) and MucR1 or MucR2.

***In vivo* phosphorylation measurements.** *In vivo* P^{32} labelling followed by immunoprecipitations (see Supplementary Fig. 1D in ref. 33) were done from cultures of a single colony of cells picked from a PYE agarose plate that was washed with M5G medium lacking phosphate and was grown overnight in M5G with 0.05 mM phosphate to an optical density of 0.3 at 660 nm (ref. 47). The strains used were as in Radhakrishnan *et al.*[33] One millilitre of culture was labelled for 4 min at 28 °C using 30 μCi of γ-[^{32}P]ATP. Following lysis, proteins were immunoprecipitated with 3 μl of antiserum to CtrA. The precipitates were resolved by SDS-PAGE, and [^{32}P]-labelled CtrA was quantified using a Storm 820 PhosphorImager and ImageQuant software version 4.0 (Molecular Dynamics) and were normalized to the relative cellular content as determined by immunoblotting of lysates. Data are from three biological replicates.

Plasmid constructions, ChIP-seq and bioinformatics analyses. Details are described in the Supplementary Methods.

References

1. Laub, M. T., Shapiro, L. & McAdams, H. H. Systems biology of *Caulobacter*. *Annu. Rev. Genet.* **41,** 429–441 (2007).
2. Murray, S. M., Panis, G., Fumeaux, C., Viollier, P. H. & Howard, M. Computational and genetic reduction of a cell cycle to its simplest, primordial components. *PLoS Biol.* **11,** e1001749 (2013).
3. Hallez, R., Bellefontaine, A. F., Letesson, J. J. & De Bolle, X. Morphological and functional asymmetry in alpha-proteobacteria. *Trends Microbiol.* **12,** 361–365 (2004).
4. Kahng, L. S. & Shapiro, L. The CcrM DNA methyltransferase of *Agrobacterium tumefaciens* is essential, and its activity is cell cycle regulated. *J. Bacteriol.* **183,** 3065–3075 (2001).
5. De Nisco, N. J., Abo, R. P., Wu, C. M., Penterman, J. & Walker, G. C. Global analysis of cell cycle gene expression of the legume symbiont *Sinorhizobium meliloti*. *Proc. Natl Acad. Sci. USA* **111,** 3217–3224 (2014).
6. Brilli, M. *et al.* The diversity and evolution of cell cycle regulation in alpha-proteobacteria: a comparative genomic analysis. *BMC Syst. Biol.* **4,** 52 (2010).
7. Rockey, D. D. & Matsumoto, A. *in*The chlamydial developmental cycle. (eds Brun, Y V. & Shimkets, L J.) 403–425 (Prokaryotic development ASM Press, 1999).
8. Christen, M. *et al.* Asymmetrical distribution of the second messenger c-di-GMP upon bacterial cell division. *Science* **328,** 1295–1297 (2010).
9. Santi, I., Dhar, N., Bousbaine, D., Wakamoto, Y. & McKinney, J. D. Single-cell dynamics of the chromosome replication and cell division cycles in mycobacteria. *Nat. Commun.* **4,** 2470 (2013).
10. Evinger, M. & Agabian, N. Envelope-associated nucleoid from *Caulobacter crescentus* stalked and swarmer cells. *J. Bacteriol.* **132,** 294–301 (1977).
11. Skerker, J. M. & Shapiro, L. Identification and cell cycle control of a novel pilus system in *Caulobacter crescentus*. *EMBO J.* **19,** 3223–3234 (2000).
12. Quon, K. C., Marczynski, G. T. & Shapiro, L. Cell cycle control by an essential bacterial two-component signal transduction protein. *Cell* **84,** 83–93 (1996).
13. Tsokos, C. G. & Laub, M. T. Polarity and cell fate asymmetry in *Caulobacter crescentus*. *Curr. Opin. Microbiol.* **15,** 744–750 (2012).
14. Wu, J. & Newton, A. Regulation of the *Caulobacter* flagellar gene hierarchy; not just for motility. *Mol. Microbiol.* **24,** 233–239 (1997).
15. Chen, J. C. *et al.* Cytokinesis signals truncation of the PodJ polarity factor by a cell cycle-regulated protease. *EMBO J.* **25,** 377–386 (2006).
16. McGrath, P. T. *et al.* High-throughput identification of transcription start sites, conserved promoter motifs and predicted regulons. *Nat. Biotechnol.* **25,** 584–592 (2007).
17. Tan, M. H., Kozdon, J. B., Shen, X., Shapiro, L. & McAdams, H. H. An essential transcription factor, SciP, enhances robustness of *Caulobacter* cell cycle regulation. *Proc. Natl Acad. Sci. USA* **107,** 18985–18990 (2010).
18. Gora, K. G. *et al.* A cell-type-specific protein-protein interaction modulates transcriptional activity of a master regulator in *Caulobacter crescentus*. *Mol. Cell* **39,** 455–467 (2010).
19. Gora, K. G. *et al.* Regulated proteolysis of a transcription factor complex is critical to cell cycle progression in *Caulobacter crescentus*. *Mol. Microbiol.* **87,** 1277–1289 (2013).
20. Klug, A. The discovery of zinc fingers and their applications in gene regulation and genome manipulation. *Annu. Rev. Biochem.* **79,** 213–231 (2010).
21. Gray, M. W., Burger, G. & Lang, B. F. Mitochondrial evolution. *Science* **283,** 1476–1481 (1999).
22. McGrath, P. T., Iniesta, A. A., Ryan, K. R., Shapiro, L. & McAdams, H. H. A dynamically localized protease complex and a polar specificity factor control a cell cycle master regulator. *Cell* **124,** 535–547 (2006).
23. Lee, J. S., Son, B., Viswanathan, P., Luethy, P. M. & Kroos, L. Combinatorial regulation of *fmgD* by MrpC2 and FruA during *Myxococcus xanthus* development. *J. Bacteriol.* **193,** 1681–1689 (2011).
24. Malgieri, G. *et al.* The prokaryotic Cys2His2 zinc-finger adopts a novel fold as revealed by the NMR structure of *Agrobacterium tumefaciens* Ros DNA-binding domain. *Proc. Natl Acad. Sci. USA* **104,** 17341–17346 (2007).
25. Mirabella, A. *et al.* Brucella melitensis MucR, an orthologue of *Sinorhizobium meliloti* MucR, is involved in resistance to oxidative, detergent, and saline stresses and cell envelope modifications. *J. Bacteriol.* **195,** 453–465 (2013).
26. Kado, C. I. Negative transcriptional regulation of virulence and oncogenes of the Ti plasmid by Ros bearing a conserved C2H2-zinc finger motif. *Plasmid* **48,** 179–185 (2002).

27. Bahlawane, C., McIntosh, M., Krol, E. & Becker, A. *Sinorhizobium meliloti* regulator MucR couples exopolysaccharide synthesis and motility. *Mol. Plant Microbe Interact.* **21,** 1498–1509 (2008).
28. Doyon, Y. *et al.* Enhancing zinc-finger-nuclease activity with improved obligate heterodimeric architectures. *Nat. Methods* **8,** 74–79 (2011).
29. Fiebig, A. *et al.* A cell cycle and nutritional checkpoint controlling bacterial surface adhesion. *PLoS Genet.* **10,** e1004101 (2014).
30. Marks, M. E. *et al.* The genetic basis of laboratory adaptation in *Caulobacter crescentus*. *J. Bacteriol.* **192,** 3678–3688 (2010).
31. D'Souza, J. M., Wang, L. & Reeves, P. Sequence of the *Escherichia coli* O26 O antigen gene cluster and identification of O26 specific genes. *Gene* **297,** 123–127 (2002).
32. Bahlawane, C., Baumgarth, B., Serrania, J., Ruberg, S. & Becker, A. Fine-tuning of galactoglucan biosynthesis in *Sinorhizobium meliloti* by differential WggR (ExpG)-, PhoB-, and MucR-dependent regulation of two promoters. *J Bacteriol* **190,** 3456–3466 (2008).
33. Radhakrishnan, S. K., Pritchard, S. & Viollier, P. H. Coupling prokaryotic cell fate and division control with a bifunctional and oscillating oxidoreductase homolog. *Dev. Cell* **18,** 90–101 (2010).
34. Llewellyn, M., Dutton, R. J., Easter, J., O'Donnol, D. & Gober, J. W. The conserved *flaF* gene has a critical role in coupling flagellin translation and assembly in *Caulobacter crescentus*. *Mol. Microbiol.* **57,** 1127–1142 (2005).
35. Ardissone, S. & Viollier, P. H. Developmental and environmental regulatory pathways in alpha-proteobacteria. *Front. Biosci.* **17,** 1695–1714 (2012).
36. Schmeisser, C. *et al. Rhizobium* sp. strain NGR234 possesses a remarkable number of secretion systems. *Appl. Environ. Microbiol.* **75,** 4035–4045 (2009).
37. Simon, R., Priefer, U. & Puhler, A. A broad host range mobilization system for *in vivo* genetic engineering: transposon mutagenesis in gram negative bacteria. *Nat. Biotechnol.* **1,** 784–790 (1983).
38. Ely, B. Genetics of *Caulobacter crescentus*. *Methods Enzymol.* **204,** 372–384 (1991).
39. Chen, J. C., Viollier, P. H. & Shapiro, L. A membrane metalloprotease participates in the sequential degradation of a *Caulobacter* polarity determinant. *Mol. Microbiol.* **55,** 1085–1103 (2005).
40. Viollier, P. H. & Shapiro, L. A lytic transglycosylase homologue, PleA, is required for the assembly of pili and the flagellum at the *Caulobacter crescentus* cell pole. *Mol. Microbiol.* **49,** 331–345 (2003).
41. Suh, S. J., Silo-Suh, L. A. & Ohman, D. E. Development of tools for the genetic manipulation of *Pseudomonas aeruginosa*. *J. Microbiol. Methods* **58,** 203–212 (2004).
42. Aldridge, P., Paul, R., Goymer, P., Rainey, P. & Jenal, U. Role of the GGDEF regulator PleD in polar development of *Caulobacter crescentus*. *Mol. Microbiol.* **47,** 1695–1708 (2003).
43. Wang, S. P., Sharma, P. L., Schoenlein, P. V. & Ely, B. A histidine protein kinase is involved in polar organelle development in *Caulobacter crescentus*. *Proc. Natl Acad. Sci. USA* **90,** 630–634 (1993).
44. Domian, I. J., Quon, K. C. & Shapiro, L. Cell type-specific phosphorylation and proteolysis of a transcriptional regulator controls the G1-to-S transition in a bacterial cell cycle. *Cell* **90,** 415–424 (1997).
45. Jacobs, C., Ausmees, N., Cordwell, S. J., Shapiro, L. & Laub, M. T. Functions of the CckA histidine kinase in *Caulobacter* cell cycle control. *Mol. Microbiol.* **47,** 1279–1290 (2003).
46. Viollier, P. H. *et al.* From The Cover: Rapid and sequential movement of individual chromosomal loci to specific subcellular locations during bacterial DNA replication. *Proc. Natl Acad. Sci. USA* **101,** 9257–9262 (2004).
47. Radhakrishnan, S. K., Thanbichler, M. & Viollier, P. H. The dynamic interplay between a cell fate determinant and a lysozyme homolog drives the asymmetric division cycle of *Caulobacter crescentus*. *Genes Dev.* **22,** 212–225 (2008).
48. Davis, N. J. & Viollier, P. H. Probing flagellar promoter occupancy in wild-type and mutant *Caulobacter crescentus* by chromatin immunoprecipitation. *FEMS Microbiol. Lett.* **319,** 146–152 (2011).
49. Viollier, P. H., Sternheim, N. & Shapiro, L. A dynamically localized histidine kinase controls the asymmetric distribution of polar pili proteins. *EMBO J.* **21,** 4420–4428 (2002).
50. Mohr, C. D., Jenal, U. & Shapiro, L. Flagellar assembly in *Caulobacter crescentus*: a basal body P-ring null mutation affects stability of the L-ring protein. *J. Bacteriol.* **178,** 675–682 (1996).
51. Figge, R. M., Divakaruni, A. V. & MreB, Gober JW. the cell shape-determining bacterial actin homologue, co-ordinates cell wall morphogenesis in *Caulobacter crescentus*. *Mol. Microbiol.* **51,** 1321–1332 (2004).
52. Hahnenberger, K. M. & Shapiro, L. Identification of a gene cluster involved in flagellar basal body biogenesis in *Caulobacter crescentus*. *J. Mol. Biol.* **194,** 91–103 (1987).

Acknowledgements

This work was supported by SNF grants no. 31003A_143660 to P.H.V. and no. 31003A_130469 to U.J. We thank Lucy Shapiro, Jim Gober, Mike Laub, Jean-Jacques Letesson, Xavier de Bolle and Matteo Brilli for materials and/or discussions.

Author contributions

C.F., S.Ar., S.K.R., J.N., S.Ab., U.J. and P.H.V. conceived and designed the experiments. C.F., S.Ar., S.K.R., J.N., S.Ab., L.T. and P.H.V. performed the experiments. C.F., S.Ar., S.K.R., J.N., S.Ab., D.M., A.F., U.J. and P.H.V. analysed the data. D.M. and A.F. contributed analytical tools. C.F., S.Ar., S.K.R., J.N., U.J. and P.H.V. wrote the paper.

Additional information

Accession codes: All ChIP-seq data was deposited in the GEO database under accession number GSE52849.

Supplementary Information accompanies this paper at http://www.nature.com/naturecommunications

Competing financial interests: The authors declare no competing financial interests.

Reprints and permission information is available online at http://npg.nature.com/reprintsandpermissions/

How to cite this article: Fumeaux, C. *et al.* Cell cycle transition from S-phase to G1 in *Caulobacter* is mediated by ancestral virulence regulators. *Nat. Commun.* 5:4081 doi: 10.1038/ncomms5081 (2014).